AN EVALUATION OF ANODE CORROSION AND GAS EMISSIONS DURING GOLD ELECTROWINNING

by

Amy Jo Chambers

A thesis submitted to the faculty of
The University of Utah
in partial fulfillment of the requirements for the degree of

Master of Science

Department of Metallurgical Engineering

The University of Utah

May 2014

The University of Utah Graduate School

STATEMENT OF THESIS APPROVAL

The thesis of **Amy Jo Chambers**

has been approved by the following supervisory committee members:

Michael L. Free	, Chair	**Oct. 21, 2013**
		Date Approved
Sivaraman Guruswamy	, Member	**Oct. 21, 2013**
		Date Approved
Sanja Miskovic	, Member	**Oct. 21, 2013**
		Date Approved

and by **Manoranjan Misra** , Chair/Dean of

the Department/College/School of **Metallurgical Engineering**

and by David B. Kieda, Dean of The Graduate School.

ABSTRACT

Gold is an important metal for a variety of uses and applications. A primary method of refining gold is electrowinning; it is used throughout the world and is becoming more and more common not only for gold processing but for other metals as well. To better understand and mitigate the negative effects of gold electrowinning, specifically anode corrosion and emissions, the effects of electrolyte composition (cyanide, chloride, hydroxide, sulfate and silicate), current density, and temperature in electrowinning cells were examined. Stainless steel electrodes were used. The emissions for gold electrowinning were also studied; specifically, ammonia and hydrogen cyanide gas evolution were examined while varying temperature, current density, and concentration of cyanide and hydroxide.

The data indicate that the greatest cause of increased anode corrosion rate is temperature. Lower temperatures examined did not cause significant corrosion except in one anode which had high cyanide and high silica. Silica is often used as a corrosion inhibitor and at low concentrations large corrosion rates were not observed, however, very high corrosion rates were observed with high concentrations of silica. At high temperature the greatest contributor to increased corrosion rate was large amounts of silica in the electrolyte. Low ion concentrations in the electrolyte showed sulfate as the greatest contributor to corrosion rate. Cyanide concentration had a small effect on corrosion rate. Corrosion was observed at varied current density, chloride, and hydroxide,

however, there was not a significant linear relationship. Significant pitting was observed in the anodes exposed to high levels of chloride.

The amount of ammonia evolved from the electrowinning cell was found to be directly proportional to the amount of cyanide loss in any given test. The largest contributor to cyanide destruction was temperature and cyanide concentration. The effects of hydroxide and current density were small and not statistically significant. The evolution of hydrogen cyanide was found to be negligible.

TABLE OF CONTENTS

LIST OF FIGURES

Figure

LIST OF TABLES

Table

ACKNOWLEDGMENTS

I would like to thank Dr. Michael Free and Dr. Michael Moats for giving me this opportunity, and especially Dr. Free for his continual advice and guidance. I would like to acknowledge Francis Elnathan for his hard work in starting the project as well as Nathan Hamilton and Daniel Azbil for their help and resourcefulness in setting up and carrying out experiments. I very much appreciate FL Smidth for funding this project. I would also like to thank my family for their love and support and my husband, Derrick, for his constant encouragement.

1 INTRODUCTION

1.1 Background

Gold has many very interesting properties that make it very useful in a wide variety of applications from jewelry to medical applications. Gold is a soft, dense, malleable, cohesive, and ductile metal. A gold leaf can be beaten so thin that it is transparent; these transparent sheets strongly reflect infrared light and are used as infrared shields in visors of heat resistant suits and in sun-visors for space suits (Mallan 1971). The University of Sheffield reports that one gram of gold can be hammered down to a sheet one meter in area. Gold is a good conductor of heat and electricity, has a melting point of 1064 ^{0}C, and forms alloys with many other metals. Alloying modifies the harness and other metallurgical properties such as the melting point.

Gold in jewelry is generally alloyed to increase its strength and sometimes for desired colors. Gold nanoparticles were used in the Middle Ages to color glass for stained glass windows in churches (Mulvaney 2003). This was done by melting gold powder into glass diffusing gold nanoparticles in the glass; these particles refract light giving the glass a desired color. The color depends upon the size and shape of the gold particles. In 1857 Faraday recognized that the color is due to the size of the gold particles (University of Sheffield 1993).

In technology colloidal gold has many applications such as electron microscopy and even tumor detection. Using Surface Enhanced Ramen Spectroscopy with gold

nanoparticles, the location of certain types of tumors can be detected (Qian 2008). Gold was first used in dentistry as early as 700-600 BC. Gold bridges were made for those who wished to show their wealth. Gold loops were fitted over natural teeth, set in place, and held by solder to keep the patient's replaced teeth in place. Biocompatibility, malleability and corrosion resistance make gold valuable in dental applications (University of Sheffield 1993). Today a typical dental gold alloy is made of gold, copper, silver and small amounts of platinum, palladium, iridium, and zinc (Phillips 1986). Before gold can be used in these applications it must be found, mined, and processed.

When humans first started mining for gold is unknown, however, gold artifacts found in Bulgaria dating back to the fifth millennia BC indicate that gold mining could be at least 7000 years old (Higham 2007). Gold has been found both in the earth's crust and its oceans; however, currently there is no economic way to extract gold from the ocean. Geologists study rock formation and mineralization and take core drill samples to find areas where the gold in the earth's crust is concentrated to an economically feasible concentration. When gold deposits are close to the surface, surface mining may be used; if the deposit is deep, underground mining may be the best mining method. Environmental, safety, and economic issues of the area are considered before any mining takes place.

Once the gold ore has been removed from the earth it must be processed to refine it and separate it from the unwanted material with which it was found. Cyanide is a ligand capable of dissolving gold into solution in a process called cyanidation which follows reaction 1.1 (International Cyanide Management Institute 2012).

$$4\,Au + 8\,CN^- + O_2 + 2\,H_2O \rightarrow 4Au(CN)_2^- + 4\,(OH)^- \qquad (1.1)$$

When the gold has dissolved into solution the excess material can be discarded and the gold can be retrieved from the cyanide solution by electrowinning.

1.2 Electrowinning

Electrowinning is an electrolytic process in which a direct current carried by free electrons drives an unspontaneous chemical reaction using two electrodes immersed in an electrolyte. The electrodes facilitate conduction of current through the electrolyte. There are two electrodes; the anode where the electrons leave the solution is positively charged while the cathode where the electrons enter the system is negative (Blount 1906). The electrolyte in gold electrowinning is a cyanide solution. The cyanide and gold in solution are in the form of ions; ions are atoms or molecules that have a differing number of electrons and protons. This electron to proton imbalance gives the atom or molecule a charge that allows the ions to carry the charge between the electrodes through the cell.

Electrowinning cells are made of nonconducting material so as to not interfere with the process. The charge of the electrodes not only carries the current through the electrolyte but also facilitates chemical reactions. Reaction 1.2 takes place at the cathode and reaction 1.3 takes place at the anode (Busch 1961) (Litz 1981) (Shreir 1963).

$$2\ Au(CN)_2^- + 2\ e^- \rightarrow 2\ Au + 4\ CN^- \quad (1.2)$$

$$H_2O \rightarrow 2\ H^+ + \frac{1}{2} O_2 + 2\ e^- \quad (1.3)$$

In the electrolyte there are two cyanide ions attracted to one gold atom. The resulting aurous dicyanide ion has an overall charge of negative one.

Yannopoulos explains the mechanism of the reactions starting with the cathode attracting positive ions to a region called the Helmholtz double layer near the surface of the cathode. The negative complex ions shown in reaction 1.2 approach the Helmholtz

layer and become polarized in the electric field of the cathode. The distribution of the ligands around the metal is distorted and the ion diffuses in to the Helmholtz layer. Within the Helmholtz layer the cyanide ligands break off the gold molecule and the gold is released as a positive cation which is deposited as the metal atom on the cathode (Yannopoulos 1991). In reaction 1.3, which takes place at the positive anode, water molecules divide into hydrogen and oxygen gas yielding two electrons. Higher gold concentration in the electrolyte yields faster rates of deposition. Electrowinning is run in alkaline electrolytes to prevent the formation of hydrogen cyanide.

Electrowinning operations are a critical part of gold recovery; one of the earliest uses was in 1842 when William Henry Fox Talbot plated gold on electrodes of a galvanic cell (Shreir 1963). Today there are several models of electrowinning cells; typical cylindrical industrial cells are placed in a cascade and connected in series. Each cell contains a pack-bed steel wool cathode; the cathode is surrounded by a steel-mesh anode. The cyanide solution is allowed to enter and flow at right angles to the direction of the current (Gupta 1990). A steel wool cathode provides a larger surface area for gold deposition, this increases efficiency and decreases time required for electrowinning. The electrolyte can be maintained at a constant gold concentration by adding gold salts in proportion to the gold-plating rate.

Solid electrodes were used in the experiments described in this study in order to better study corrosion of the anodes. Insoluble anodes made of rolled gold or stainless steel may be used. Insoluble anodes are popular because they minimize capital investment (Yannopoulos 1991). Once the reaction has finished the gold is removed from the cathodes followed by smelting to produce gold bullion.

Anodes are typically permanent and require cleaning and maintenance. High current densities may cause particles to flake off the anode. This can cause higher current densities in some areas of the anode which in turn causes changes in current density in areas on the cathode. Such changes cause low current efficiency and lower quality of the metal plating on the cathode (Moskalyk 1999). Anodes may also corrode, reducing the life of the anode.

1.3 Corrosion

Corrosion in metals is caused when a metal is transformed from a metallic to an oxidized state. The corrosion product can be similar if not the same as the natural oxidized state of the metal in an ore body and is more thermodynamically stable than the pure metal. This stable oxidized state of a metal usually contains oxide or sulfide. When ore is refined, energy is used to remove oxygen, sulfur, and unwanted elements until a mostly pure metal remains. With time, water, and proper conditions the refined metal returns to a more stable, oxidized state as a mineral such as a metal oxide or sulfide. Depending on the kinetics of this reaction and the environment of the metal, the corrosion process may be slow enough that the metal is essentially stable. Figure 1.1 illustrates the relationship of time and energy with a typical metal (Chandler 1998).

In this study corrosion rates are reported as a time averaged weight loss, implying a uniform corrosion rate; however, few metals and alloys corrode uniformly, corrosion is more likely to be localized (i.e., pitting, crevice corrosion, etc. is the rule). The corrosion rates reported in this study are relative and for the purposes of comparison between different electrolyte solutions, current densities, and temperatures.

There are many processes which cause corrosion. Pitting corrosion is a highly localized attack of the metal that creates pits of varying depth, width, and number. Pitting may often lead to complete perforation of the metal with little or no general corrosion of the surface. Crevice corrosion is similar to pitting corrosion in its localized nature but is associated with crevices. Stainless steels and some nickel-base alloys are particularly susceptible to this form of corrosion. These types of attacks are the result of accelerated corrosion due to flow of solids, liquids or gases (Craig 1995).

While electrolysis is the exchange of ions to create a pure metal, corrosion is the exchange of ions to form the more stable and less pure form of the metal. In an electrowinning cell, corrosion and electrolysis may take place simultaneously. Figure 1.2 shows corrosion of an anode taking place (Chandler 1998). The electrolyte has an effect on the type and kinetics of corrosion reactions. The presence of chlorides and sulfides has been shown to promote corrosion because they increase the conductivity of water, and because they can contribute to metal oxide film instability.

The annual cost of corrosion in the world is estimated to be about two and a quarter trillion dollars (Hays 2013). Fontana lists multiple pathways that corrosion follows to cause financial problems. Corroded parts and machinery must be purchased over again, and downtime required of a plant to fix or replace corroded parts causes a loss of production. Corrosion may cause loss of product if the corrosion causes leaks in containers, tanks, or pipelines; leaks may also damage the environment. Corrosion may cause loss of efficiency in a process, for example, corrosion products accumulated on heat exchanger tubing decreases the efficiency of heat transfer (Fontana 1986).

Understanding corrosion will lead to better methods of corrosion prevention, which could save industries as well as consumers a significant cost.

In this study corrosion is examined in an electrowinning cell with stainless steel electrodes. When immersed in water over time stainless steel forms a loose brown corrosion product caused by the oxidation of iron called rust. At high temperatures the rate of oxidation increases. The water line is especially susceptible to corrosion because it is an area that has a three phase boundary; the metal, electrolyte solution, and the atmosphere. Oxygen diffuses rapidly through the thin layer of solution at this boundary, resulting in a rapid attack. Water line attack is particularly noted in water containing sulfate, bicarbonate, and dissolved oxygen (Shreir 1963).

Corrosion rates differ depending on ions present in the electrolyte and electrolysis parameters such as temperature. Some ions are known to increase corrosion rates while others may slow corrosion rates. High concentrations of chloride and sulfate ions are known to increase corrosion rates. The effect of high concentrations of silica ion, cyanide, and hydroxide ions is not well understood. High temperature generally increases corrosion rates; however, in the presence of certain conditions it may inhibit corrosion. Overly high current density is known to cause poor metal deposition, but the relationship of current density and corrosion is not clearly understood.

The aim of the anode corrosion experiments in this study is to examine the effects of ion concentration in the electrolyte (Cyanide [NaCN], chloride [NaCl], sulfate [Na_2SO_4], hydroxide [NaOH] and silicate [Na_2SiO_3]) and electrolysis parameters (current density and temperature) on the corrosion of commercial anode samples. There have been many studies conducted dealing with different electrolyte compositions and corrosion.

This study will verify what is known and explore further the concentrations at which certain ions begin to cause increased corrosion rates.

Cyanide has been shown to dissolve silver anodes but there is little literature exploring the effect cyanide has on stainless steel. The literature focuses on the oxidizing effect electrolysis has on cyanide rather than the effect of cyanide on corrosion. Gold recovery was not examined in this study, however, other studies have shown excess free cyanide ions in electrolyte decrease recovery (Brandon 1987). This study will examine the anodes in electrolytes containing various cyanide concentrations.

Halogen salts are known to be corrosive to stainless steel because of the tendency to cause local film failure and pitting. Pitting is promoted in aerated or mildly acidic oxidizing solutions. Chlorides generally are more aggressive than the other halides in causing pitting (Craig 1995). Chlorides also cause pitting in steel reinforcements in concrete; because pitting tends to cause mechanical failures by fatigue or stress corrosion cracking it is considered by some to be the most costly form of corrosion. Pitting in aqueous chloride solutions depends on the rate of dissolution of the metal in areas where the passive film has failed. The electrolyte penetrates the passive film and hydrolysis of the dissolving metal cations creating an acidified area in which pit growth occurs. The acidification process can overcome high alkalinity. Even in concrete which has a pH of about thirteen, the corrosion site can be reduced to a pH of about five (Newman 2010).

Hu el al. found that stainless steels immersed in chloride solutions exhibit crevice corrosion behavior. The corrosion was divided into three stages: an incubation period, a rapid development stage and a stable development stage. Crevice corrosion was observed to develop at the crevice bottom and then spread to the whole electrode (Hu 2011),

(Pistorius 1992). Maier and Frankel found pitting in 304 stainless steel exposed to droplets of chloride solution. The pits initiated sooner under small droplets because of faster evaporation and therefore higher chloride concentration of the droplets (Maier 2010). Yang el al. found that in magnesium submerged in solutions of chloride and sulfate the chloride destroyed the corrosion film causing pitting corrosion while the sulfate caused shallow general corrosion covering a larger surface area. Sulfate was found to cause more and faster weight loss than the chloride (Yang 2010). It is well established that high chloride concentration will often cause significant pitting corrosion in metals; this study will focus on the effect of smaller concentrations of chloride on the corrosion behavior in an electrolytic cell.

Sulfate enhances oxidation to Fe(III) (Cekerevac 2012). In the presence of sulfate, ferrous metals will form a membrane of ferric hydroxide. The membrane will restrict passage of oxygen so that the oxidation will be limited to the formation of a magnetite or hydrated magnetite tubercle. This reaction will cause liberation of acid. Reaction 1.4 shows the liberation of acid.

$$Fe^{2+} + 2\,Fe^{3+} + 4H_2O \rightarrow Fe_3O_4 + 8H^+ \qquad (1.4)$$

Liberation of acid causes the interior of the tubercle to become acidic which causes the magnetite to act as a cathode. The corrosion rate is accelerated by the trapped acid between the anode and the magnetite cathode. Acid solutions are more corrosive than alkaline solutions; however, there is a passivation point in alkaline solutions above which severe pitting may occur although overall corrosion is reduced (Shreir 1963).

When sulfate is added to the system the potential changes. A black precipitate has been observed in some studies. The precipitate was identified through chemical testing as

ferrous oxide which oxidized to ferric oxide in air (Smith 2011). In sulfate systems under alkaline solutions ferrous hydroxide and ferric hydroxide were found (Simard 2001). In sewer systems sulfur is oxidized by bacteria, ultimately forming sulfuric acid which is very corrosive. The literature does not specify a particular concentration at which corrosion becomes a problem; this study will investigate the effects of a variety of sulfate concentrations on anode corrosion.

Sodium hydroxide is also known as caustic soda. It is used to control the pH in an electrowinning solution. The solution was kept above a pH of 11 in a gold electrowinning solution because of the tendency of cyanide to make hydrogen cyanide gas in acidic solutions. Hydroxide concentration increases as electrowinning goes on, however, evidence suggests hydroxide does not largely affect the rate of corrosion. All stainless steels resist general corrosion by sodium hydroxide at temperatures below about 66 C (Craig 1995). Shrier reports alkaline waters as less corrosive than acid or neutral water. Shrier also reports iron having less weight loss in more alkaline solutions over five days than more acidic solutions, although the temperature and exact pH are not reported.

There are many studies on the benefits of silica with regards to preventing corrosion. Fumed silica is used to decrease corrosion in a variety of applications. When it is added to concrete the strength and resistivity are increased. The increase in resistivity causes a decrease in the corrosion of the reinforcement steel bars (Dotto 2004). Silica is sometimes added to water systems to inhibit corrosion in pipes.

Rushing et al. studied the effects of silica on oxidation of iron from Fe^{2+} to Fe^{3+} by adding 30 mg/L of ferrous iron to aerated water in multiple tests. Solutions of water, silica in the water, and silica as well as hydroxide in the water were examined. With no

silica the ferrous iron was 95% oxidized in thirty minutes. When silica was added to the water only 66 and 60% of the ferrous iron were oxidized. When pH was held constant at 8.1 by adding 1 M NaOH, slower rates of oxidation were again found in solutions containing silica. More silica contributed to slower oxidation in every test. The silica slowed oxidation in water with or without hydroxide (Rushing 2003). Rushing et al. further examined the effect of silica in water on the corrosion rates of cast iron pipes. Increased silica content was found to increase the concentration of particulate iron in the water, increase the extent of tuberculation, and decrease the long term corrosion rate. The weight of the tubercles was included in the final mass of the iron samples.

Cekerevac et al. found that the anode will absorb silicate on its surface which suppresses the formations of Fe(III) compounds. This supports growth of a dense layer of Fe(II) hydroxide and mixed Fe(II, III) oxides (Cekerevac 2012). In the literature most studies examine the effect of relatively low concentrations of silicate; in this study low as well as high concentrations of silicate are tested.

Temperature also effects corrosion; corrosion at high temperatures by oxidation and sulfidation can take the form of uniform attack or pitting. Stress-corrosion cracking of some stainless steels can occur at higher temperatures (Craig 1995). Lower temperatures in pipes sometimes yield greater corrosion rates (Rushing 2003). Temperature can influence many water chemistry parameters such as dissolved oxygen solubility, oxidation rates, and activity coefficients. Each of these factors can affect the iron corrosion rate. Gases dissolve more readily in cooler temperatures; this could contribute to more dissolved oxygen and therefor more iron oxidation. High temperatures give energy needed for a reaction to take place; this could also promote corrosion.

Temperature can have different effects on corrosion of the same metal depending on the chemicals present. This study will vary temperature in high and low sulfate and silica concentrations to better understand the effect of temperature on these solution parameters.

Current density is the electric current per unit area in SI units, and in this study it is measured in amperes per square meter. When the current density is changed in this study the electrode size is not, therefore, the electric current must be changed. In copper electrowinning when the current density is too high the deposit begins to become rough and impure. As the current density approaches the limiting current density the deposit can become powdery and hydrogen gas can discharge. This occurs because the electrode potential becomes more negative and the concentration of metal ions decreases close to the cathode (Ettel 1975). Current density will be varied as one of the parameters of the study to determine its influence on anode corrosion.

1.4 Emissions

In an electrowinning cell a byproduct of the oxidation and reduction reactions occurring at the electrodes is the emission of gases. Reduction at a cathode yields hydrogen gas from reaction 1.5, while oxidation at the anode yields oxygen gas from reaction 1.6.

$$2H^+(aq) + 2e^- \rightarrow H_2(g) \quad (1.5)$$

$$2H_2O(l) \rightarrow O_2(g) + 4H^+(aq) + 4e^- \quad (1.6)$$

The volume of gas generated during any given experiment can be calculated using Faraday's law (1.7) the ideal gas law (1.8) and three equations (1.9, 1.10, 1.11) relating amperes, time, coulombs, Faraday's constant and moles of electrons. In this study

Faradays law and the ideal gas law are used to find the volume of gas generated in the electrowinning cell at 88 ºC or 361 K.

$$m = \frac{M*I*t}{z*F} \tag{1.7}$$

m = the mass in grams of the gas evolved, M = the molar mass of the gas, I = the current in amperes, t = the time in seconds the electrolysis was running, z = the electrons transferred, F = Faraday's constant.

$$V = \frac{n*R*T}{P} \tag{1.8}$$

V = the volume, n = the number of moles, R = the ideal gas constant, T = the temperature in kelvin, P = pressure.

$$\text{Amperes * time = Coulombs} \tag{1.9}$$

$$\text{96,485 coulombs = 1 Faraday} \tag{1.10}$$

$$\text{1 Faraday = 1 mole of electrons} \tag{1.11}$$

Using these equations and the data from the study found in Table 1.1, the volume of hydrogen and oxygen gas can be found. First the amperes are calculated in equation 1.12.

$$85\ cm^2\ x\ \frac{30\ A}{10000\ cm^2} = 0.255\ Amperes \tag{1.12}$$

Using Faraday's law the mass of hydrogen and oxygen gas in grams is found in equations 1.13 and 1.14, respectively.

$$\frac{2.0158\frac{g}{mol}*\ 0.255A*\ 14400\ s}{96{,}485\frac{C}{mol}*\ 2} = 0.0384\ g\ H_2 \tag{1.13}$$

$$\frac{31.9989\frac{g}{mol}*\ 0.255A*\ 14400\ s}{96{,}485\frac{C}{mol}*\ 4} = 0.3045\ g\ O_2 \tag{1.14}$$

The mass of gas generated is converted to moles and the volume in liters of H_2 and O_2 gas generated is calculated in equations 1.15 and 1.16, respectively.

$$\frac{\frac{0.0384\ \text{g}}{2.0158\ \frac{\text{g}}{mol}}\ H_2 * 0.08206\ \frac{L*atm}{mol*K} * 361\ K}{1\ atm} = \mathbf{0.563\ L\ H_2} \quad (1.15)$$

$$\frac{\frac{0.3045\ \text{g}}{31.9989\ \frac{\text{g}}{mol}}\ H_2 * 0.08206\ \frac{L*atm}{mol*K} * 361\ K}{1\ atm} = \mathbf{0.281\ L\ O_2} \quad (1.16)$$

This generation of hydrogen and oxygen gas in electrolysis is well known; the purpose of the off-gases tests in this study was to quantify the amount of ammonia and hydrogen cyanide evolving from a laboratory electrowinning (EW) cell. The effect of cyanide concentration, hydroxide, temperature and current density on the gaseous emissions was examined.

Hydrogen cyanide, also known as hydrocyanic acid, is the most toxic form of cyanide. Formation occurs when cyanide is protonated. Hydrogen cyanide is a very volatile species with a boiling point at 25.7 °C. Hydrogen cyanide is particularly dangerous because inhalation of the gas can be fatal depending on the concentration. Hydrogen cyanide, however, does not readily convert to the gaseous phase. Table 1.2 shows the reported time until death for different concentrations of exposure to hydrogen cyanide gas (World Health Organisation 2004). Cyanide in water is also very toxic to wildlife, especially fish which have a very low cyanide tolerance. Values in ppm are approximate calculations from mg, where ppm = mg/m^3 / gram molecular weight x 24.45 (molar volume of air at standard temperature and pressure).

Other studies have not tested the amounts of hydrogen cyanide formed from electrowinning cells. The pK_a for HCN dissociation reaction is 9.24 at 25 °C, therefore, at pH greater than 9.24, cyanide dominates and less than 9.24, hydrogen cyanide is the

dominant species. The pK_a indicates that if the solution stays above a pH of 9.24 the risk of hydrogen cyanide gas formation is low. A hydrogen cyanide detector was still used to ensure the safety of the researchers and a solution was made to capture any gas that may form. All electrowinning tests with cyanide solutions were performed in a hood for additional safety.

Ammonia exists naturally in animals and the environment, and is essential for many biological processes. At room temperature it is a colorless gas with a pungent odor. When ammonia gas is inhaled it is irritating and corrosive, high concentrations cause a burning sensation in the nose, throat, and respiratory tract. Low concentrations can cause coughing, and nose and throat irritation (Agency for Toxic Substance and Disease Registry 2004). Gaseous ammonia released into the environment stays in the atmosphere for about 24 hours and generally deposits within 700 to 1000 meters of its source. Deposition of ammonia in the environment can contribute to eutrophication of surface water, soil acidification, fertilization of vegetation, changes in ecosystems, and smog in cities. Eutrophication is a result of nutrient pollution into natural waters and promotes excessive plant growth and decay and may cause reductions in water quality (Colorado State University 2008).

The formation of hydrogen cyanide gas has been studied extensively. In industry precautions are taken to ensure the gas does not form and harm both employees and environment. The formation of ammonia from electrowinning cells has not been studied specifically. The mechanism of hydrolysis of cyanide has been studied and ammonia has been reported as a byproduct. The quantity of ammonia produced in electrolysis has not been captured and quantified in previous studies.

In this study the formation of hydrogen cyanide or ammonia gases would result from reactions involving cyanide in an electrowinning cell. In the case of ammonia formation, cyanide will degrade into ions before forming other molecules. Cyanide degradation has been utilized in treatment of waste water containing cyanide. Waste water containing cyanide must be treated before it is reintroduced into the environment. Studies have been done to understand the cyanide degradation process as well as to find ways to optimize these treatment processes. Ho et al. found that cyanide concentrations dropped from 1400 mg/L to below 20 mg/L in 4 to 20 hours of electrolytic treatment at 5-13 kw h/kg (Ho 1990).

Experiments done by A. Valiūnienė et al. indicate that increased alkalinity (pH=13) in the electrolyte of an electrolytic process does not decrease the amount of cyanide ion degraded. The minimum pH for effective cyanide destruction was found to be 11.3. The cyanide degradation reaction differs depending on the electrode material. Platinum, titanium with a thin layer of platinum on the surface, and stainless steel anodes where used. The stainless steel anodes were the least effective for cyanide ion destruction. Increased temperature of the electrolyte was found to increase cyanide destruction with the titanium electrodes, the temperatures tested were 10, 20, 30, and 40 ^{o}C.

Cyanide reduction occurs in the region of hydrogen gas evolution at the negative electrode. Thermal destruction of cyanide may occur by hydrolysis or by combustion. At a pH of 8, under up to 100 bars of pressure, and between 140 and 200 ^{o}C cyanide hydrolysis occurs rapidly by reaction 1.17.

$$CN^- + 2\,H_2O \rightarrow HCOO^- + NH_3 \qquad (1.17)$$

In the presence of nitriles the ammonia and formate can be destroyed to form nitrogen, carbon dioxide gas, and water. In this study nitriles were not used, therefore it is expected that ammonia will be the byproduct of the cyanide destruction (Valiūnienė July 2013) (Dzombak 2006).

The rate of free cyanide hydrolysis shown by equation 1.17 is very slow at room temperature. Dzombak et al. reports that the rate increases about three-fold for every 10 ^{0}C increase in temperature. This reaction takes place readily in alkaline conditions, high temperatures and high pressure (Dzombak 2006). Free cyanide can also be oxidized by chloride, hypochlorite, ozone and hydrogen peroxide. Under neutral to alkaline conditions, cyanide oxidation may form cyanate CNO^- and ammonia. Cyanate is relatively nontoxic. Alkaline chlorination oxidation for cyanide is used for rapid treatment of free cyanide in water.

The formation of acid mist is studied extensively for copper and zinc electrowinning circuits. Gold electrowinning, however, is carried out in alkaline solutions and acid mist is not formed. There is little literature dealing with the emission of ammonia or hydrogen cyanate in gold electrowinning. The information available focuses on the destruction of cyanide in electrolysis reactions for water treatment purposes.

Although the formation of hydrogen cyanide gas is unlikely, the quantity of gas produced will be measured to verify what is known as well as to ensure the safety of the researchers. The formation of ammonia has been observed in cyanide hydrolysis, this study will seek to better understand the quantity of ammonia gas formed and the parameters that influence formation in the electrowinning cell. The influence of varying

the amount of hydroxide, cyanide, current density, and temperature on the amount of gas generated will also be examined.

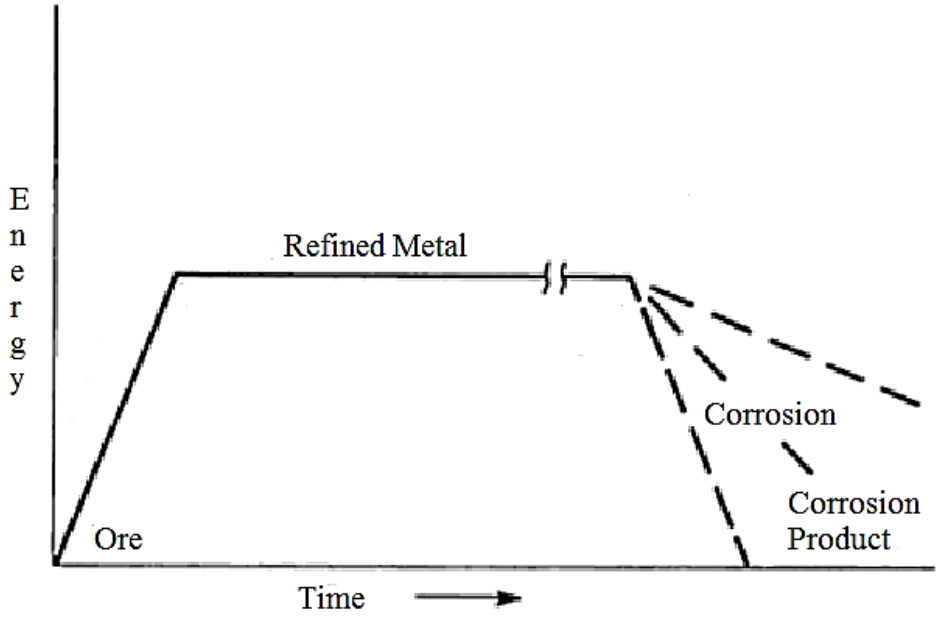

Figure 1.1: Time versus energy of metals (adapted from Chandler 1998).

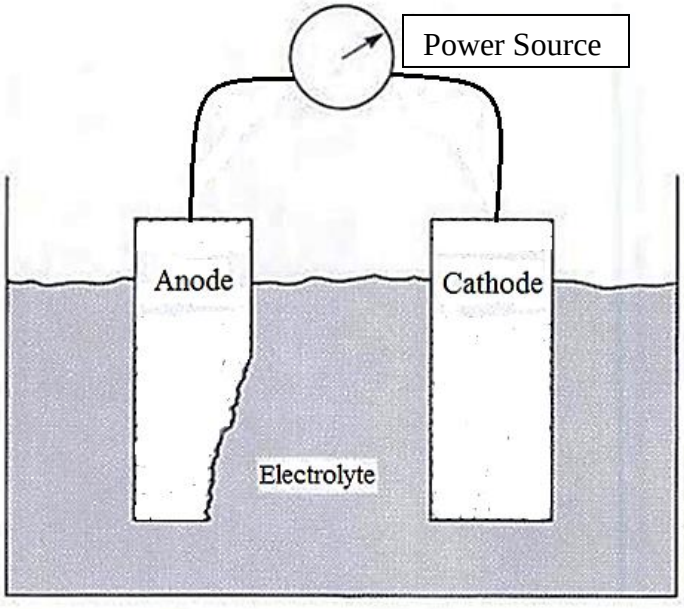

Figure 1.2: Corrosion of an anode in electrowinning (adapted from Chandler 1998).

Table 1.1: Data used to calculate volume of gas evolved.

Effective area of anode	Current Density	Time	Mass H_2	Mass O_2
85 cm^2	30 A/m^2	14400 sec	2.0158 g/mol	31.9989 g/mol

Table 1.2: Time of death following cyanide exposure data source: (W.H.O 2004).

Dose Inhaled		**Time to Death**
mg/m^3	**ppm**	
150	135	30 minutes
200	180	10 minutes
300	270	Immediate

2 EXPERIMENTAL PROCEDURES

2.1 Anode Corrosion Experiments

Trial runs for the anode corrosion experiments were started in October 2011 to work out potential problems in the experimental apparatus. Full operational conditions for anode corrosion experiments were started in mid-February 2012.

The oil bath shown in Figure 2.1 has two compartments. Each compartment has capacity for four one liter electrolytic cells allowing for a total of eight experimental conditions to be tested simultaneously. Each reactor was filled with one liter of the electrolyte solution under study. An anode and a cathode were then inserted into the solution through slits in the cell cover. A fresh sample electrode is shown in Figure 2.2. The metal used for the anodes was type 304 stainless steel purchased from McMaster-Carr. The type 304 stainless steel has a hardness of 150-241 Brinell and yield strength of 30,000 to 40,000 psi. The metal is annealed, cold finished and meets ASTM Standard number A240 (McMaster-Carr n.d.).

The anodes were in operation for six weeks for each test except when the test duration was shortened due to extreme corrosion occurring earlier than anticipated (for example, in the study of sulfate). The dimensions of the stainless steel electrode samples were approximately 16.5 × 2.5 cm with some minor variation. The cells were inserted into the oil bath at the desired operating temperature which varied depending on the experiment. A stirring rod with an impeller was inserted between the anode and cathode and operated continuously for the duration of each test. The cells were connected in

series to an external power supply. A data logger was connected to each cell to monitor the voltage and time in case of power fluctuation during the experiments.

The primary form of data retrieval involved the use of Tracer DAQ Pro software. Each individual electrode was wired to the receiving mechanism, which transferred the information to the computer via USB. The software was set to receive data at a rate of .01 Hz. This was maintained for the length of the experiment. The accuracy of the acquired data was crosschecked using a volt ohm meter (VOM) and a resistor of known resistance. The resistor was placed in the series of cells, and then the VOM was used to measure the voltage across the resistor. Ohm's law was then used to measure the accuracy of the current being displayed on the power source. Figure 2.3 shows voltage data taken from a six-week experiment from January 6-February15, 2013. Figure 2.3 is an example of data from three hours of testing.

The solution volumes and cyanide concentrations were tested daily and maintained by adding additional solution as needed. Initially a drip system was put into place where hospital IV bags containing cyanide solution were connected to each cell and set to drip slowly to replace the liquid and cyanide ions that were lost. This system did not function correctly and a top off system was incorporated. The cells had a mark at the one liter line to make top off simple, every morning and evening the volume of liquid lacking was manually added to the cells through small holes in the lid that were covered by electrical tape except when cells were being filled.

In order to know how much cyanide to add to the cells each day the amount of cyanide present in the cell was titrated daily during preliminary tests. When the amount of cyanide lost each day was determined a standard solution of cyanide was made and

was added when the cells were topped off. The solutions were titrated on a regular basis during tests to ensure the correct amount of cyanide was maintained in each cell.

Cyanide concentration was determined by titration using 0.1 M $AgNO_3$ with KI as indicator. Hydroxide concentration was determined by titration using 1 M HCl with methyl orange as indicator. Daily cyanide concentration variations were very high during the cyanide study. In order to mitigate the variation the area of the electrodes was reduced by half which reduced the current supplied to each compartment of cells by half.

Hydroxide monitoring was very difficult from the onset of the corrosion experiments because hydroxide concentration increased daily. In order to avoid very high hydroxide concentrations the electrolyte was replaced three times each week during the hydroxide investigation. During the chloride investigation an attempt was made to measure changes in the chloride concentration by first destroying cyanide in the system, then titrating for the remaining chloride. Meaningful results were not obtained and did not follow any discernible trend, so this procedure was discontinued. No attempt was made to measure the changes in sulfate concentration. The electrolyte under study was replaced every two weeks to mitigate the effects of soluble species variation on the test results.

The amount of corrosion was quantified by measuring the difference in mass of each anode before and after testing. After six weeks of operation the anodes typically had deposits that adversely affected the mass loss measurements. These deposits were tested using EDAX (Emission Dispersion Analysis of X-ray) and were found to contain mostly calcium. Because only deionized water was used in making solutions it is believed the deposits came from the wear of the plastic stir rods. The deposits were removed in order

to find an accurate mass change strictly due to the corrosion of the anode. The removal was done following the ASTM G1 standard for cleaning corrosion test specimens (ASTM 2003). The anode samples were immersed in dilute nitric acid for multiple timed cleaning cycles. The mass was measured after each cleaning cycle and plotted in a graph similar to Figure 2.4. The deposits have successfully been removed when the slope approaches zero. Equation 2.1 is used to find the actual final weight after cleaning.

$$Total\ mass\ loss = measured\ mass\ loss - mass\ of\ corrosion\ product \quad (2.1)$$

2.2 Emissions Tests

The EW cell was scaled down in design to simulate an industrial EW cell. The scale down was achieved by maintaining the same industrial solution flow rate per surface area of electrode and the same solution flow rate per surface area of the cell. The anode area is 43 cm^2 and the flow rate is 1.2 L/min through the 1.2 liter cell. The optimum flow rate was determined through preliminary tests by measuring the gas capture at five different flow rates of the peristaltic pump used. The results of these tests are shown in Figure 2.5. A 20-liter storage vessel containing electrolyte was heated to the desired temperature and insulated tubing was used to pump the electrolyte from the storage vessel through the cell and back into the storage vessel. The tests were conducted for four hours at the desired temperature.

The gases evolved in the EW cell were measured by sampling the air space above the cell. A sampling port was situated directly above the anode and the solution line; the anode was positioned between two cathodes as is common in industrial operations. A tube connected the sampling port to a condenser held in place above the EW cell by a clamp. The emissions tests setup is shown in Figures 2.6 and 2.7. Initially the condenser

was connected to a Y-connector splitting into two Erlenmeyer flasks. One flask contained an acidified solution designed to trap ammonia, and the other flask contained a solution designed to trap hydrogen cyanide gas.

Because hydrogen cyanide was negligible the flasks containing solutions to trap hydrogen cyanide were discontinued. In initial tests the amount of ammonia gas captured varied greatly due to gas leakage, so a secondary container was used to enclose the entire cell and reduce leakage.

The number of Erlenmeyer flasks required to collect each sample of gas evolved was determined experimentally. Roughly 80% of the total ammonia capture was found in the first flask and 20% in the second flask. Thus, nearly all of the ammonia was captured by two flasks of scrubbing solutions. 0.1M HCl was used to capture the ammonia gas similar to the Kjeldahl ammonia process (Harris 2003). The HCl solution that had captured the ammonia during the four-hour test time was titrated using sodium hydroxide. Evolved gases were drawn through the capture flasks by a vacuum pump. The flasks containing the scrubbing solution were filled with glass beads and placed in an ice bath to improve gas absorption.

It was observed that much of the cyanide degradation was due to heat in the storage vessel. Degradation in the storage vessel presented a problem in the mass balance of the emissions captured from the cell. Consequently, a second series of collection flasks and a second condenser were assembled to collect the gas evolved from the storage vessel. A valve was added to the second collection flask series to enable the adjustment of the flow rate allowing equal flow through each flask series. The Appendix contains a detailed description of how the emissions tests were set up and operated.

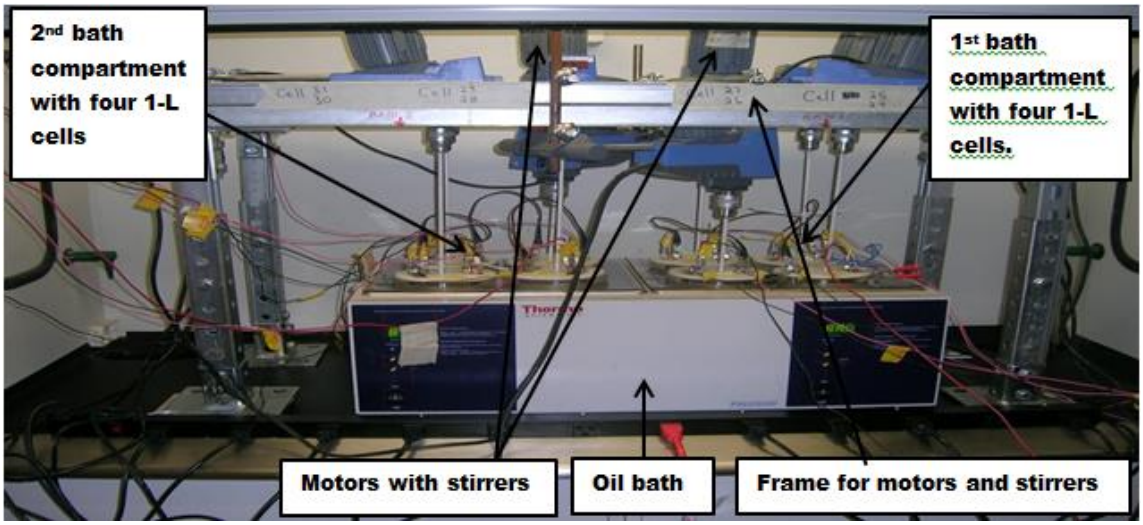

Figure 2.1: Anode corrosion setup.

Figure 2.2: Electrode before testing.

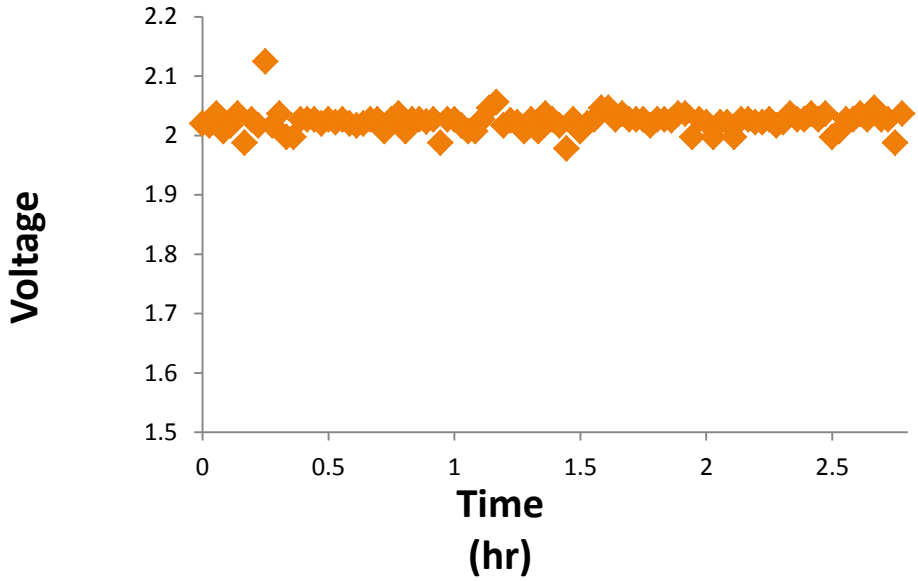

Figure 2.3: Three hour sample of electrowinning cell voltage data.

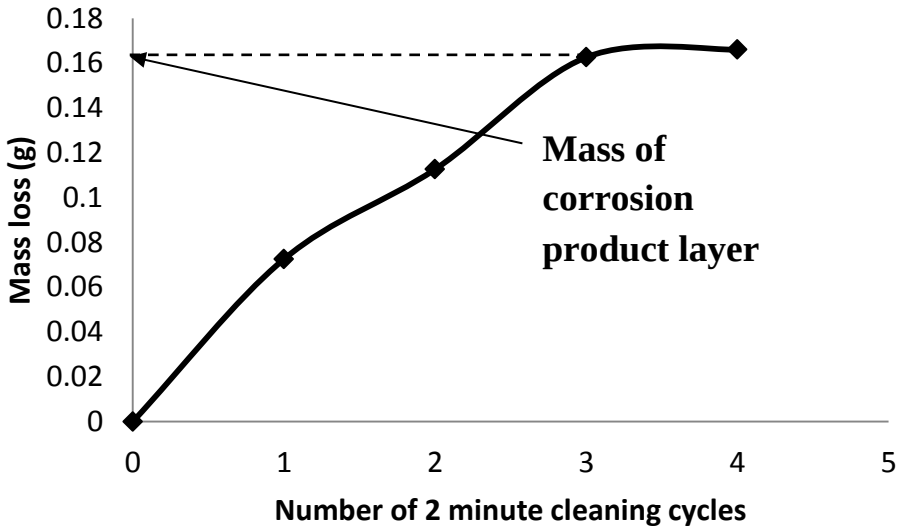

Figure 2.4: Graph constructed during cleaning of anode 18.

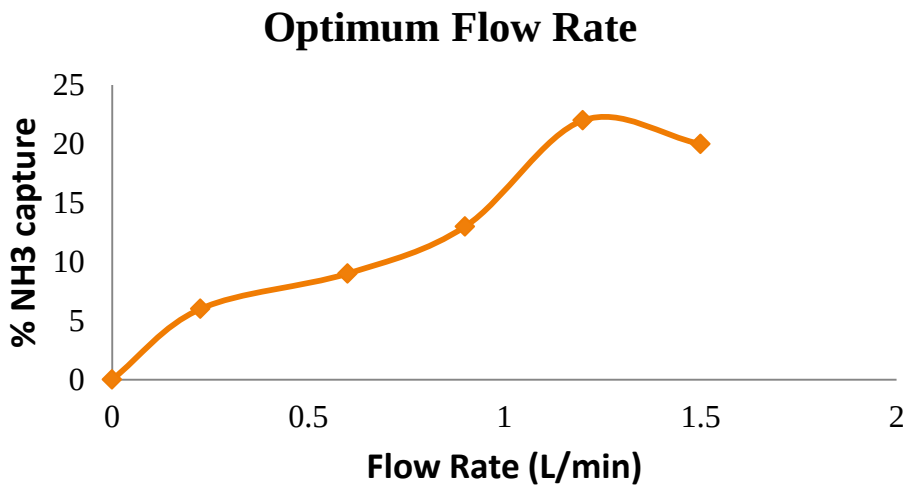

Figure 2.5: Determination of optimum flow rate.

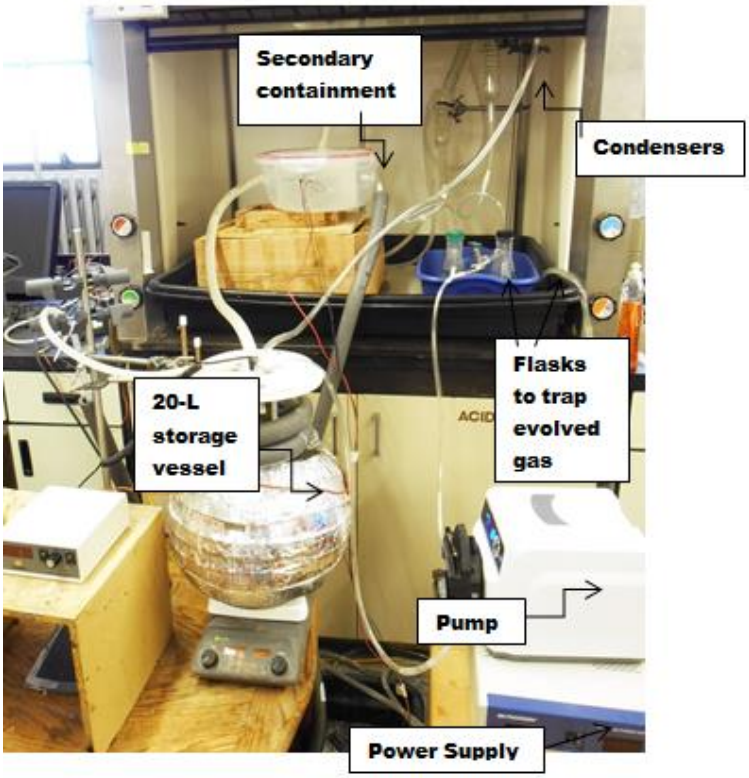

Figure 2.6: Complete emissions test setup.

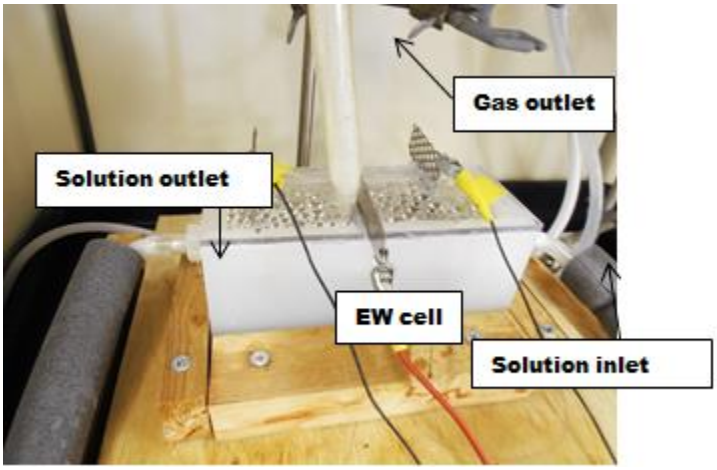

Figure 2.7: Electrowinning cell without secondary containment.

3 RESULTS

3.1 Anode Corrosion

3.1.1 Effect of NaCN on Anode Corrosion

The effects of the sodium cyanide on the anode corrosion are presented in Table 3.1. Visual inspection of the images shown in Figures 3.1 and 3.2 appears to corroborate the results of Table 3.1 For example, tests 2 and 3 shown in Figure 3.1 appear to be the only anodes that showed a significant amount of corrosion in the cyanide concentration study. Table 3.1 also shows that anodes 2 and 3 are the only ones that show significant corrosion. However, it should be noted that cyanide concentrations fluctuated very significantly during initial testing, as can be seen in Figure 3.3. The temperature for every cell was 88°C and the chloride was 0.04 g/L.

Modifications were made to the experimental procedure for subsequent tests, and this dramatically improved the control of cyanide concentration as shown in Figure 3.4. The voltage in the electrolysis system is expected to increase gradually over time as the anodic over-potential of the system increases. An example plot for anodes 0 and 1 for two weeks duration is shown in Figure 3.5. The voltage increases gradually over the test duration with some noise registering in the plots. Tests to determine the effect of sodium cyanide on anode corrosion were repeated later.

3.1.2 Effect of NaCl on Anode Corrosion

The anode corrosion results from the testing at different chloride levels are reported in Table 3.2. Images of corroded anodes obtained from the chloride testing are shown in Figure 3.6. The temperature for all tests was 88 °C and the cyanide concentration was three grams per liter.

Anode 13 showed the most corrosion of the chloride tests. In order to better see the corrosion taking place a cross section of the anode was mounted in epoxy then viewed under a microscope. Figure 3.7 shows the image captured; small pitting was observed. The pit shown in Figure 3.7 is 51.6 microns into the electrode. Assuming the pit will grow linearly through the anode and the pits grow from both sides; the anode can be expected to cause complete penetration through the anode in 36 weeks. If the pit grows only from one side, the anode can be expected to fail in 72 weeks.

3.1.3 Effect of Na_2SO_4 on Anode Corrosion

Anode corrosion results obtained from the sulfate investigation are presented in Table 3.3. Increasing sulfate concentration appears to have a linear effect on corrosion. The unusually low corrosion value for anode 18 is not well understood. Temperature for all cells was 88 °C and cyanide concentration was 3 g/L.

Anodes 22 A and 23 A, as seen in Figure 3.8, were tested in the highest sulfate concentration (74 g/L) and failed (fell apart) in 28 days. The anodes were replaced by new electrodes labeled 22 B and 23 B. The new anodes were tested in 45 g/L sulfate concentration, however, corrosion was not observed in anodes (22 B and 23 B) in the 14 days testing period. Also, anode 20 A was replaced by anode 20 B on day 40 after failing. Corrosion was not observed in anode 20 B when the sulfate investigation ended on day

42. Because anode 23 showed the most corrosion in the sulfate solution, a cross section was cut and mounted in epoxy. Figure 3.9 shows the cross section magnified. A large amount of pitting was observed.

3.1.4 Effect of NaOH on Anode Corrosion

Anodes 24 through 31 were tested to evaluate the effect of different hydroxide concentrations. Anodes 26 and 27 were tested for a lower level of sulfate than had previously been examined. In all tests the concentration of hydroxide was shown to increase with time. In order to keep the hydroxide levels as close as possible to the initial concentrations, the solutions were changed three times a week rather than every 2 weeks. All cells ran for 42 days at 88 ^{o}C, A/m^2 was 30. The result of this test set is shown in Table 3.4, while Figure 3.10 shows the anodes.

3.1.5 Effect of Na_2SiO_3 and Current Density on Anode Corrosion

Table 3.5 show the corrosion observed from variance of silica concentration and current density. The data show a distinct trend for increasing corrosion with increasing silicate that becomes very high at the highest level of silicate. After 2 weeks the corrosion was very high for Anode 32 with no silicate, although after the anode was replaced in the cell by a new anode, corrosion for the following 4 weeks was very low. Figure 3.11 shows the anodes. The temperature for all cells was 88 ^{o}C; there was 10 grams of sodium hydroxide in the electrolyte of each cell and no sodium sulfate.

A cross section of Anode 35 was cut and mounted in epoxy. Figure 3.12 shows the magnified cross section and confirms the aggressive corrosion caused by the presence of silicate. Figure 3.13 shows the anodes that were subjected to varying current density.

3.1.6 Effect of Lower Temperature (71° C) on Anode Corrosion

Table 3.6 illustrates the corrosion measured in the anodes after exposure to the electrolyte containing silica and sulfate as used previously but at a lower temperature. Figure 3.14 shows the anodes in sulfate solution. Figure 3.15 shows the magnified cross section of Anode 42, which shows negligible corrosion. Figure 3.16 shows corrosion in anodes exposed to electrolyte containing silicate. The largest amount of corrosion is seen in Anode 47 which had the highest concentration of silicate examined. Current density was 30 A/m^2 for all cells and sodium hydroxide was 10 gram per liter for each cell.

3.1.7 Effect of Low Na_2SiO_3 and Na_2SO_4 on Anode Corrosion

In order to discover a lower level at which corrosion becomes significant, low concentrations of silica and sulfate were examined at 88° C. Table 3.7 shows the results of the study. After three weeks it was determined that lower concentrations should be examined. Anodes 53 and 54 where replaced with 53B and 54 B and the electrolyte solution was switched to an even lower concentration solution. Anodes 48 and 49 were repeats of previous cyanide effect testing in which the cyanide concentration was not adequately controlled. Figure 3.17 shows the anodes after testing, cleaning, and weighing. The current density was 30 A/m^2 and the temperature was 88 ^oC for all cells. Ten grams of sodium hydroxide were in the electrolyte for all cells.

3.1.8 Intermediate Temperature Anode Testing

The corrosion effects of high and low concentrations of Na_2SiO_3 and Na_2SO_4 were evaluated at intermediate temperatures to find the relationship between temperature and corrosion at differing concentrations of Na_2SiO_3 and Na_2SO_4. This test was undertaken because previous results indicated that temperature, Na_2SiO_3, and Na_2SO_4

concentrations had the greatest effect on corrosion. The current density for each cell was 30 A/m^2; the electrolyte for each cell contained 3 grams of sodium cyanide and 10 grams of sodium chloride. Table 3.8 illustrates the corrosion observed and Figure 3.18 shows the anodes after testing and cleaning.

3.1.9 Low and Mixed Na_2SiO_3 and Na_2SO_4 Anodes

Some tests were repeated in the last six week test set. Table 3.9 shows the corrosion observed for the conditions tested. Each cell was kept at 88 ^oC with 30 A/m^2 current density; the electrolyte in each cell contained ten grams of sodium hydroxide. Na_2SiO_3 and Na_2SO_4 were included in the same cell for the first time in this test set. The anodes are shown in Figure 3.19. Less corrosion was observed in the cells with both Na_2SiO_3 and Na_2SO_4 present; this could indicate the ions have a synergistic interaction with each other that reduces corrosion.

3.2 Emissions Testing

The objective of the emissions testing was to determine the amount of gas evolved, specifically hydrogen cyanide and ammonia gas. Hydrogen cyanide was found in very small quantities in preliminary tests; the amount was negligible as shown in Table 3.10. Therefore, testing for HCN emission was discontinued for subsequent tests. The emissions test variables and ranges with their associated NH_3 capture and CN^- loss are presented in Table 3.11. Values that vary from the standard conditions are bold.

A few two-hour tests were also conducted to examine the effect of temperature alone on cyanide degradation. Each two-hour test was performed as described in the procedure section except the power supply was not turned on in tests performed without electrolysis. Table 3.12 shows the results of these tests.

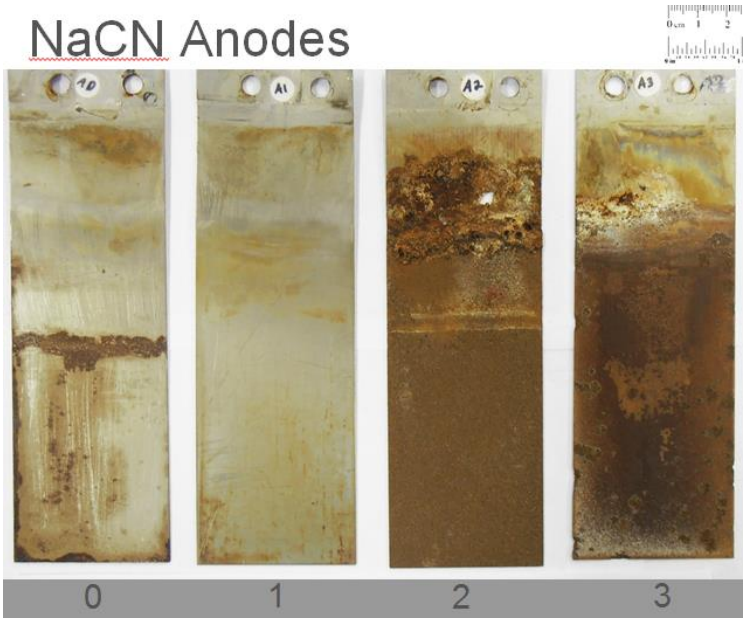

Figure 3.1: Anodes 0-3 correspond to results in Table 3.1.

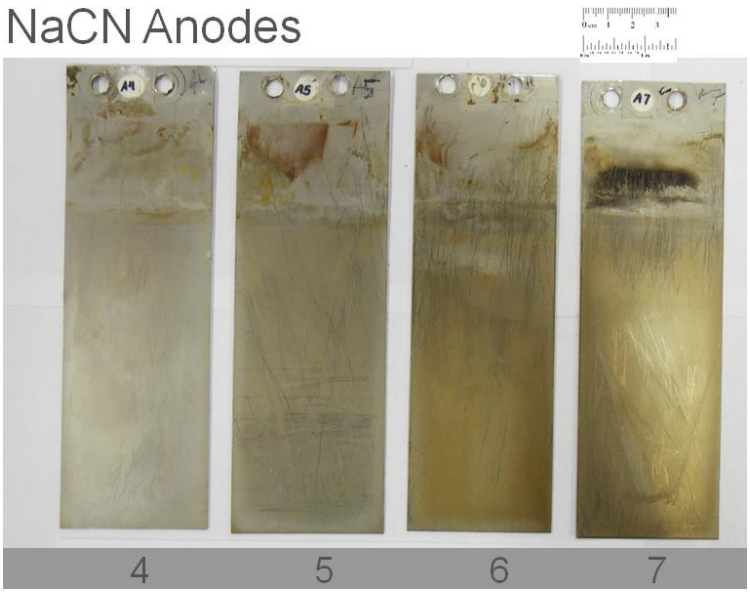

Figure 3.2: Anodes 4-7 correspond to data in Table 3.1.

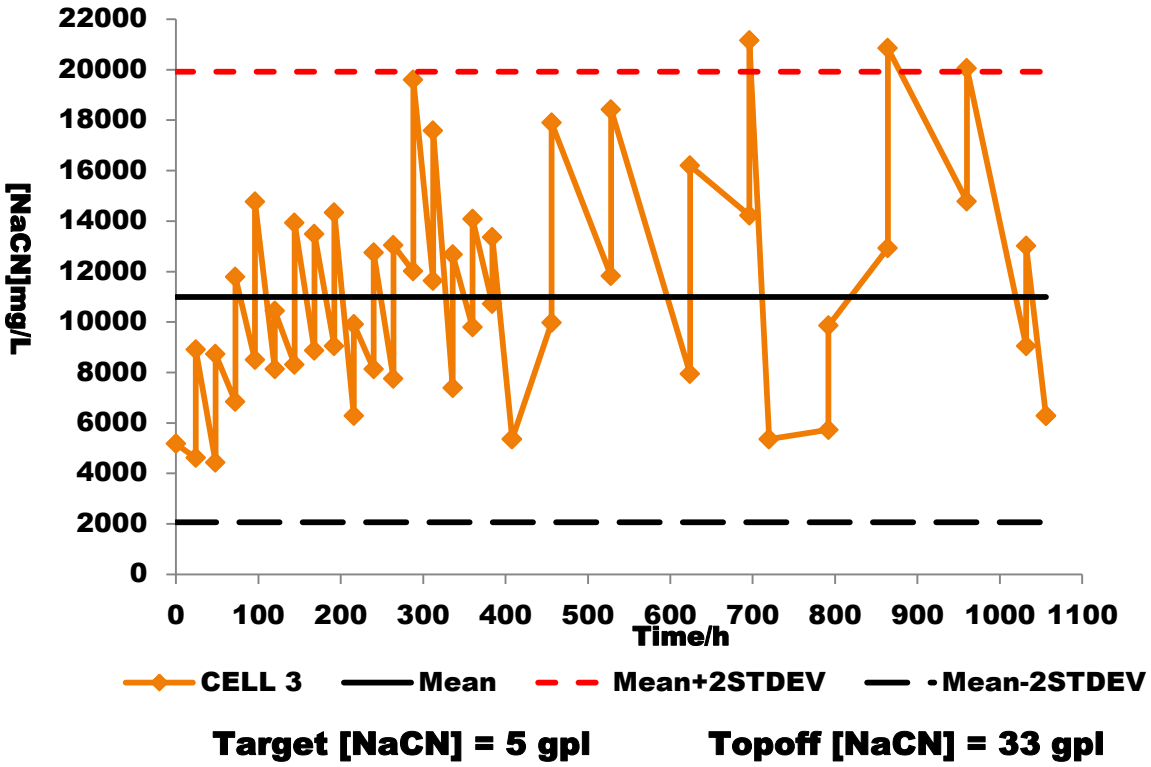

Figure 3.3: High variability of cyanide concentration.

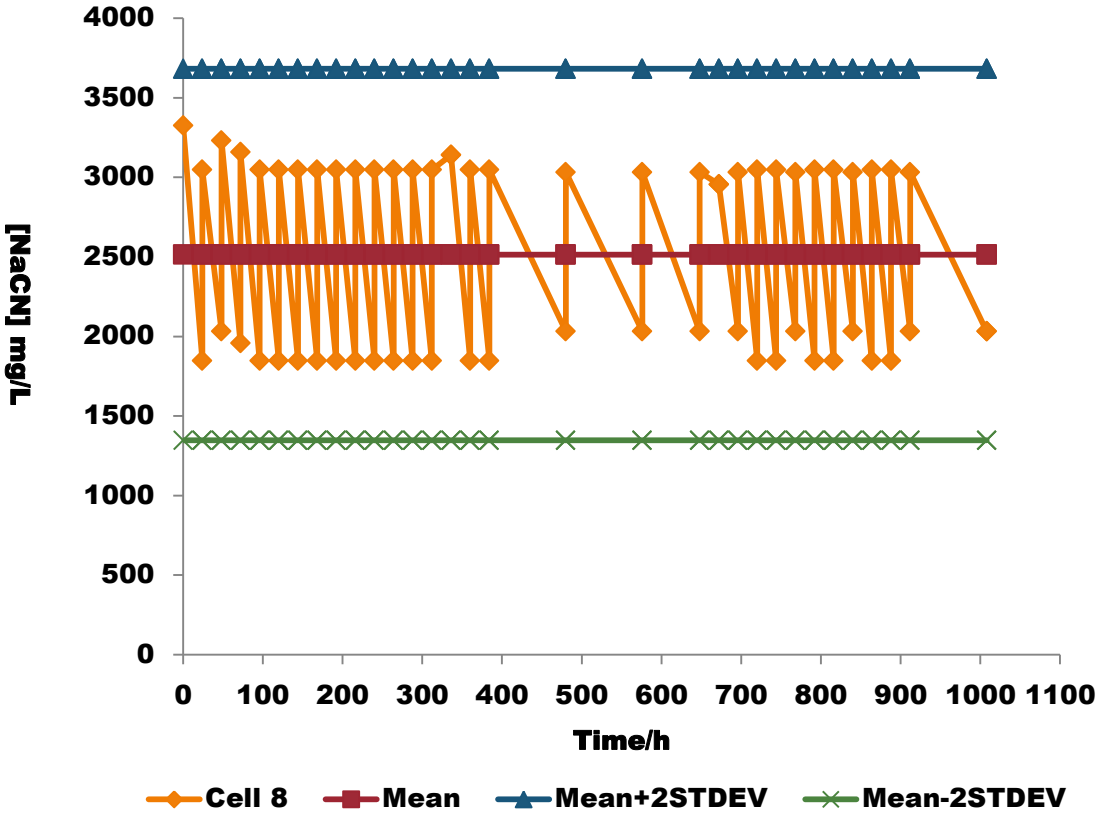

Figure 3.4: Stable control of cyanide concentration.

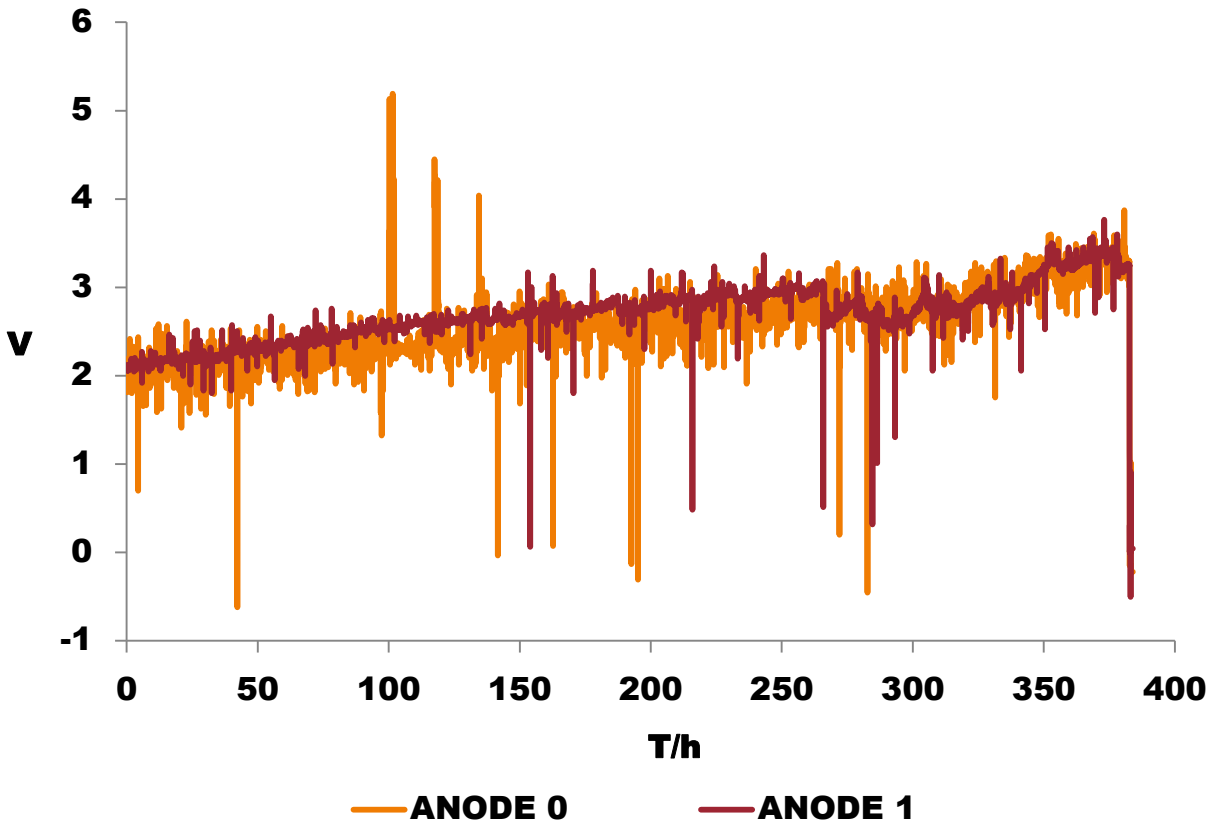

Figure 3.5: Voltage-time plot showing anodes 0 and 1 over a two week period.

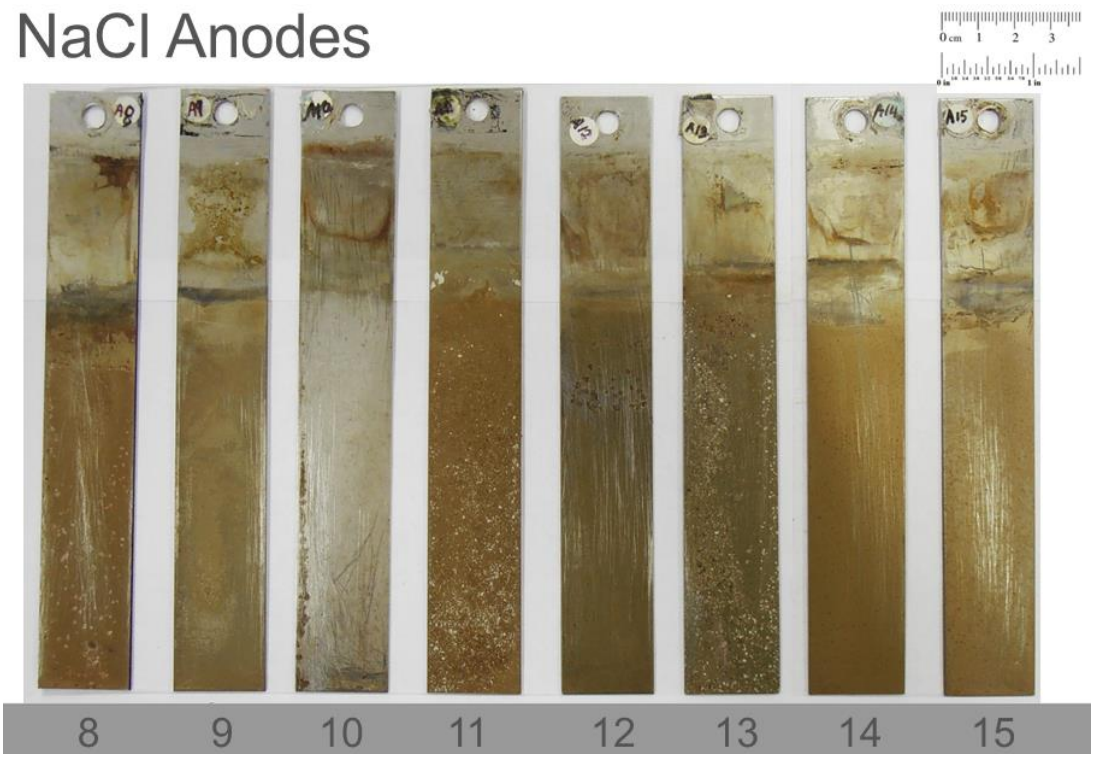

Figure 3.6: Anodes 8-15 correspond to data presented in Table 3.2.

Figure 3.7: Anode 13 magnified.

Figure 3.8: Anodes 16-23 correspond to data presented in Table 3.3.

Figure 3.9: Large pitting observed in cross section of anode 23.

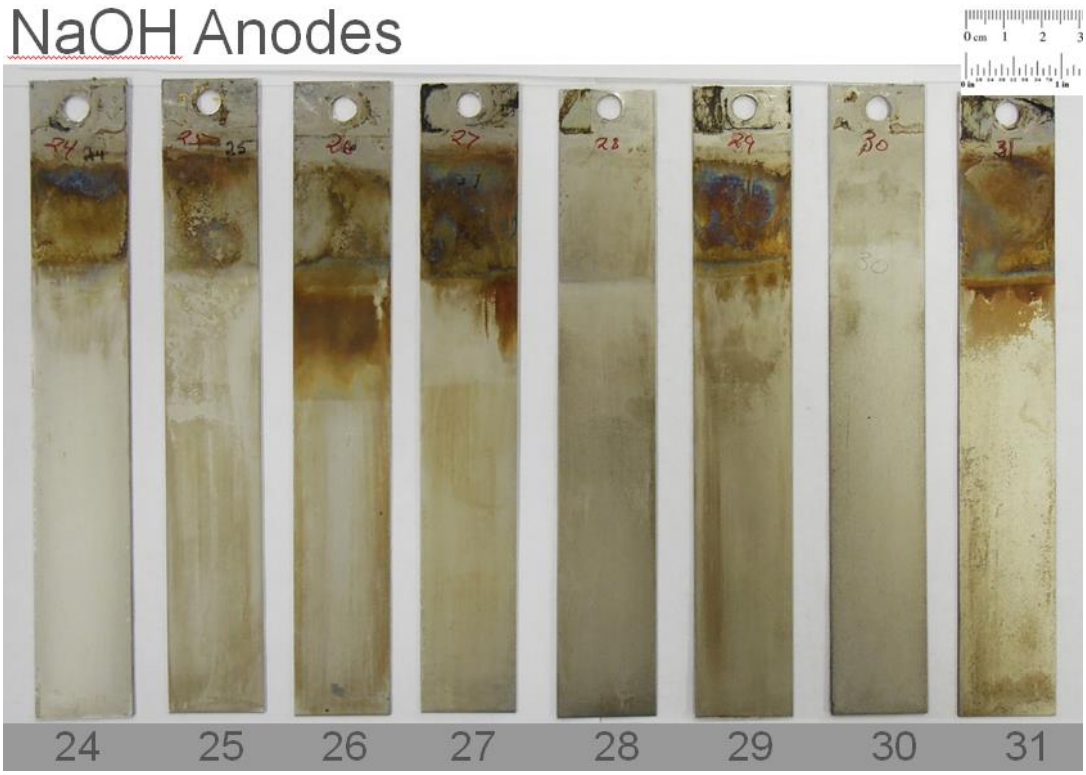

Figure 3.10: Anodes 24-31 correspond to the data in Table 3.4.

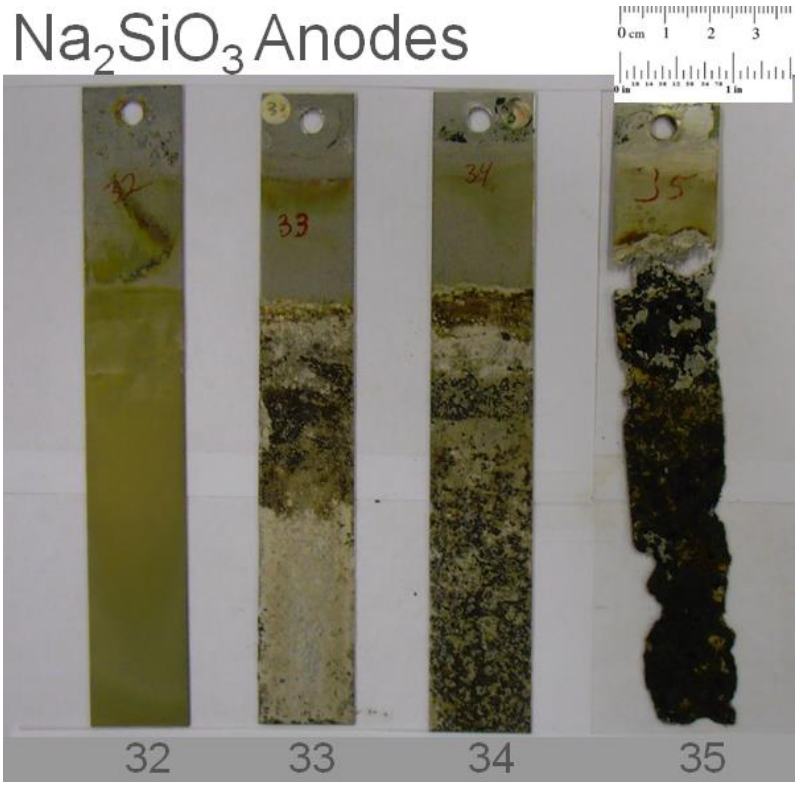

Figure 3.11: Anodes 32-35 correspond to data in Table 3.5.

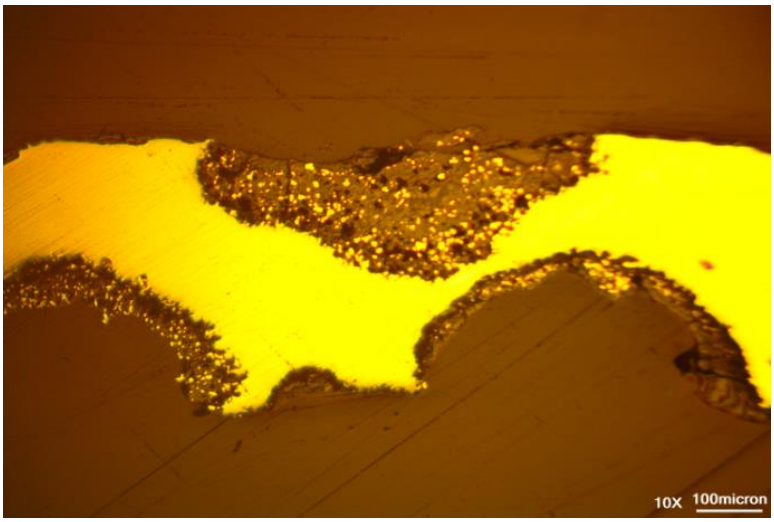

Figure 3.12: Cross section of anode 35.

Figure 3.13: Anodes 36-38 correspond to data in Table 3.5.

Figure 3.14: Anodes tested in electrolyte containing Na_2SO_4 at 71°C.

Figure 3.15: Cross section of anode 42.

Figure 3.16: Anodes 45-47 correspond to data in Table 3.6.

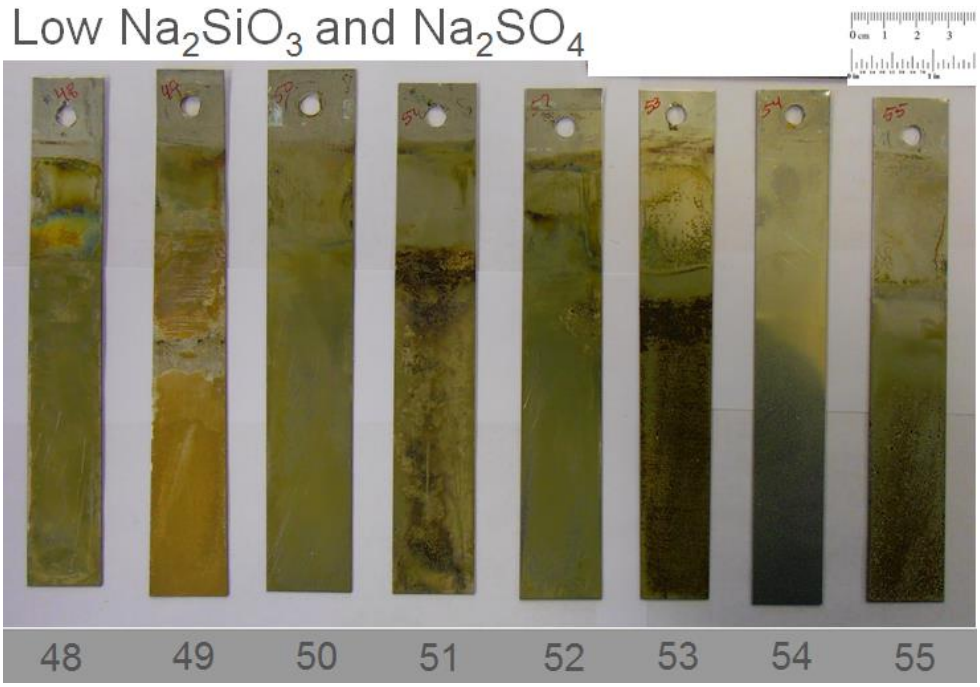

Figure 3.17: Anodes 48-55 correspond to data in Table 3.7.

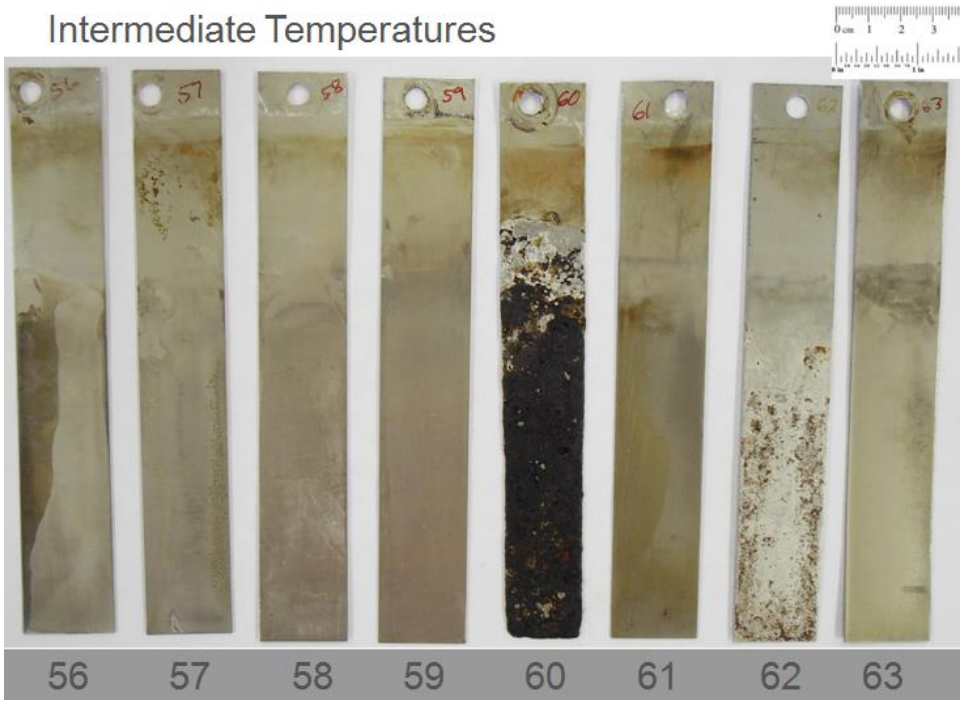

Figure 3.18: Anodes 56-63 correspond to data in Table 3.8.

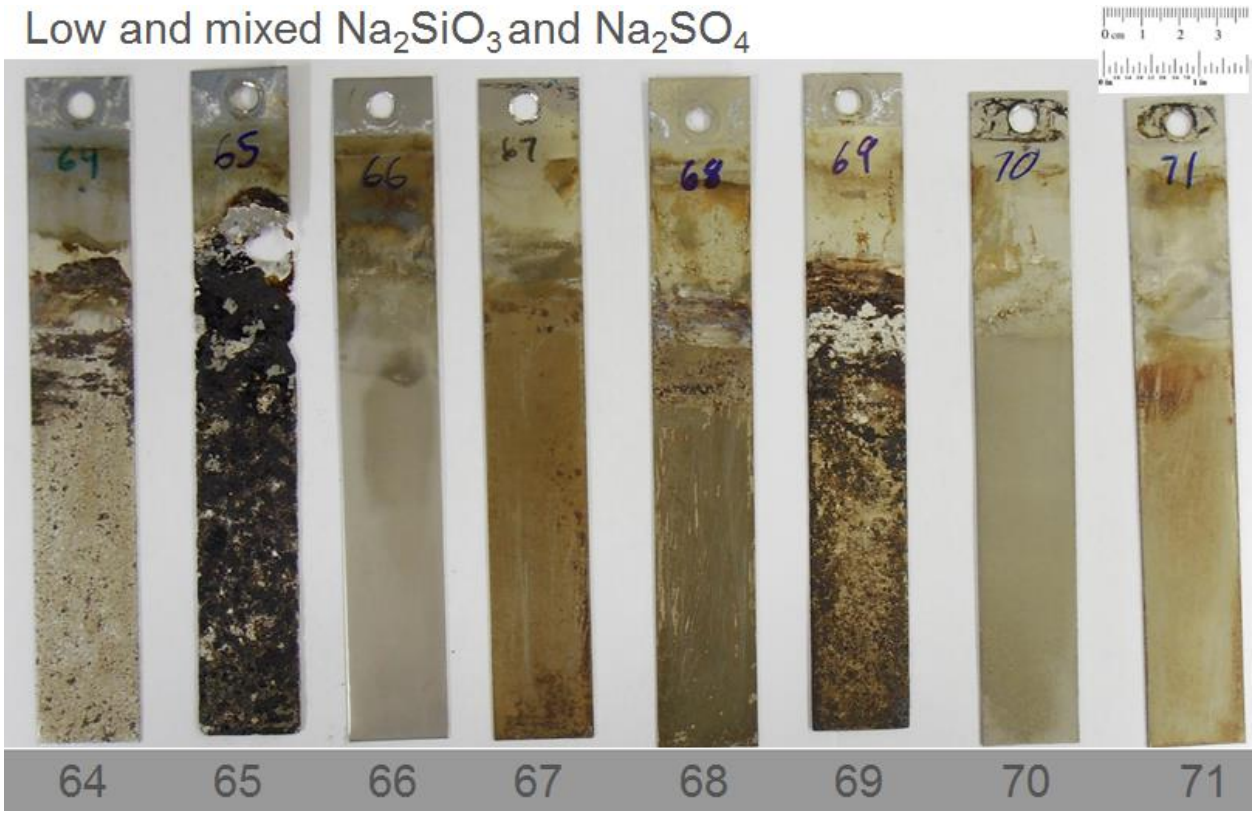

Figure 3.19: Anodes 64-71 correspond to data in Table 3.9.

Table 3.1: Corrosion results from varied cyanide concentration tests.

Test ID	A/m^2	NaCN (g/L)	Na_2SO_4 (g/L)	NaOH (g/L)	Na_2SiO_3 (g/L)	Δ Mass (grams)	Area (m^2)	Time (day)	Corr. Obs. (g/m^2/day)
0	30	0	0	10	0	0.1367	0.0060	42	0.5396*
1	30	0	0	10	0	0.0084	0.0061	42	0.0328*
2	30	5	0	10	0	8.707	0.0062	42	33.5019*
3	30	5	0	10	0	3.4092	0.0064	42	12.7388*
4	30	10	0	10	0	0.0259	0.0062	42	0.0994
5	30	10	0	10	0	0.0259	0.0064	42	0.0958
6	30	18	0	10	0	0.0365	0.0060	42	0.1456
7	30	18	0	10	0	0.0729	0.0059	42	0.2934

* Indicates inadequate cyanide control

Table 3.2: Corrosion results from the varied chloride concentration tests.

Test ID	A/m^2	NaCl (g/L)	Na_2SO_4 (g/L)	NaOH (g/L)	Na_2SiO_3 (g/L)	Δ Mass (grams)	Area (m^2)	Time (day)	Corr. Obs. (g/m^2/day)
8	30	**0.04**	0	10	0	0.021	0.0030	42	0.1658
9	30	**0.04**	0	10	0	0.0023	0.0030	42	0.0186
10	30	**0.08**	0	10	0	0.0275	0.0030	42	0.2176
11	30	**0.08**	0	10	0	0.0077	0.0030	42	0.0616
12	30	**0.16**	0	10	0	0.0293	0.0030	42	0.2365
13	30	**0.16**	0	10	0	0.1236	0.0030	42	0.9976
14	30	**0.33**	0	10	0	0.0064	0.0031	42	0.0493
15	30	**0.33**	0	10	0	0.0172	0.0030	42	0.1388

Table 3.3: Corrosion results from varied sulfate concentration tests.

Test ID	A/m^2	NaCl (g/L)	Na_2SO_4 (g/L)	NaOH (g/L)	Na_2SiO_3 (g/L)	Δ Mass (grams)	Area (m^2)	Time (day)	Corr. Obs. (g/m^2/day)
16	30	0.04	**0.7**	10	0	2.4539	0.0031	42	19.0437
17	30	0.04	**0.7**	10	0	4.9393	0.0031	42	37.6931
18	30	0.04	**3**	10	0	0.0325	0.0030	42	0.2588
19	30	0.04	**3**	10	0	1.1726	0.0031	42	8.9484
20**	30	0.04	**15**	10	0	3.6018	0.0029	40	31.3200
21	30	0.04	**15**	10	0	0.201	0.0031	42	1.5691
22***	30	0.04	**74**	10	0	6.7406	0.0030	28	80.2452
23***	30	0.04	**74**	10	0	6.7158	0.0029	28	83.8636

: Anode 20 A ran for 40 days and failed while 20 B ran for 2 days and showed no sign of corrosion at a sulfate concentration of 15 g/L. * Anodes 22 A and 23 A failed in 28 days at a sulfate concentration of 74 g/L. The replacements anodes (22 B and 23 B) examined in 45g/L sulfate concentration did show signs of corrosion in 14 days.

Table 3.4: Corrosion results from varied hydroxide concentration tests.

Test ID	NaCN (g/L)	NaCl (g/L)	Na_2SO_4 (g/L)	NaOH (g/L)	Na_2SiO_3 (g/L)	Δ Mass (grams)	Area (m^2)	Corr. Obs. ($g/m^2/day$)
24	3	0.04	0	**5**	0	0.054	0.0030	0.4286
25	3	0.04	0	**5**	0	0.0322	0.0029	0.2621
26	3	0.04	0.37	**10**	0	0.0584	0.0029	0.4754
27	3	0.04	0.37	**10**	0	0.0721	0.0029	0.5971
28	3	0.04	0	**15**	0	0.0885	0.0029	0.7185
29	3	0.04	0	**15**	0	0.0802	0.0030	0.6419
30	3	0.04	0	**20**	0	0.0559	0.0031	0.4328
31	3	0.04	0	**20**	0	0.0631	0.0031	0.4926

Table 3.5: Data from varied silicate and current density tests.

Test ID	A/m^2	NaCN	NaCl	Na_2SiO_3	Δ Mass (grams)	Area (m^2)	Time (day)	Corr. Obs. ($g/m^2/day$)
32	30	3	0.04	0	0.4965	0.0030	14	11.8610
33	30	3	0.04	**1.87**	0.969	0.0028	42	8.1669
34	30	3	0.04	**3.74**	0.353	0.0031	42	2.6878
35	30	3	0.04	**5.61**	8.3219	0.0031	42	63.5066
36	**20**	3	0.04	0	0.151	0.0028	42	1.2650
37	**25**	3	0.04	0	0.1486	0.0032	42	1.1154
38	**35**	3	0.04	0	0.0228	0.0033	42	0.1621
39	30	**5**	0.04	0	0.2672	0.0033	42	1.9002

Table 3.6: Test data for the variation of silicate and sulfate at 71 °C.

Test ID	Temp (°C)	NaCN (g/L)	NaCl (g/L)	Na_2SO_4 (g/L)	Na_2SiO_3 (g/L)	Δ Mass (grams)	Area (m^2)	Time (day)	Corr. Obs. (g/m^2/day)
40	71	3	0.04	**0.7**	0	0.0188	0.0030	42	0.1492
41	71	3	0.04	**3**	0	0.016	0.0027	42	0.1392
42	71	3	0.04	**15**	0	0.0196	0.0031	42	0.1493
43	71	3	0.04	**0.37**	0	0.021	0.0027	42	0.1874
44	71	3	**0.33**	0	0	0.0279	0.0032	42	0.2100
45	71	3	0.04	0	**1.87**	0.0148	0.0028	42	0.1259
46	71	3	0.04	0	**3.74**	0.0118	0.0032	42	0.0873
47	71	18	0.04	0	**5.61**	0.1974	0.0030	42	1.5667

Table 3.7: Data for tests with low Na_2SiO_3 and Na_2SO_4 at 88 °C.

Test ID	A/m^2	NaCl (g/L)	Na_2SO_4 (g/L)	Na_2SiO_3 (g/L)	Δ Mass (grams)	Area (m^2)	Time (day)	Corr. Obs. (g/m^2/day)
48	30	0.04	0	0	0.0145	0.0026	42	0.1328
49	30	0.04	0	0	0.091	0.0026	42	0.8276
50	30	0.04	0	**0.9**	0.0091	0.0033	42	0.0650
51	30	0.04	0	**0.4**	0.0894	0.0029	42	0.7322
52	30	0.04	0	**0.1**	0.0236	0.0029	42	0.1972
53 A	30	0.04	**0.5**	0	0.0109	0.0032	20	0.1678
53 B	30	0.04	**0.001**	0	0.0663	0.0027	22	1.1015
54 A	30	0.04	**0.25**	0	0.0065	0.0024	20	0.1371
54 B	30	0.04	**0.05**	0	0.0018	0.0027	22	0.0307
55	30	0.04	**0.1**	0	0.0566	0.0027	42	0.4969

Table 3.8: Data from selected testing with Na_2SiO_3 and Na_2SO_4 at 76.7 and 82.3 °C.

Test ID	Temp (°C)	NaCl (g/L)	Na_2SO_4 (g/L)	Na_2SiO_3 (g/L)	Δ Mass (grams)	Area (m^2)	Time (day)	Corr. Obs. (g/m^2/day)
56	**76.7**	0.04	**15**	0	0.012	0.0030	42	0.0964
57	**76.7**	0.04	**0.7**	0	0.0072	0.0029	42	0.0602
58	**76.7**	0.04	0	**5.61**	0.0001	0.0030	42	0.0008
59	**76.7**	0.04	0	**1.87**	0.0021	0.0030	42	0.0166
60	**82.3**	0.04	**15**	0	4.0699	0.0029	42	33.3342
61	**82.3**	0.04	**0.7**	0	0.0088	0.0027	42	0.0766
62	**82.3**	0.04	0	**5.61**	0.1626	0.0030	42	1.3061
63	**82.3**	0.04	0	**1.87**	0.0006	0.0030	42	0.0048

Table 3.9: Data for testing with low and mixed Na_2SiO_3 and Na_2SO_4 additions.

Test ID	NaCN (g/L)	NaCl (g/L)	Na_2SO_4 (g/L)	Na_2SiO_3 (g/L)	Δ Mass (grams)	Area (m^2)	Time (day)	Corr. Obs. (g/m^2/day)
64	3	0.04	**0.5**	0	0.2552	0.0032	42	1.8988
65	3	0.04	**0.25**	0	5.1027	0.0032	42	38.3500
66	3	0.04	**0.1**	0	0.0041	0.0031	42	0.0315
67	3	0.04	0	**1.5**	0.0209	0.0032	42	0.1580
68	3	0.04	0	**0.75**	0.0498	0.0031	42	0.3794
69	3	0.04	0	**0.25**	0.5626	0.0031	42	4.3919
70	3	0.04	**0.5**	**1.5**	0.0026	0.0031	42	0.0198
71	3	0.04	**0.25**	**0.75**	0.0162	0.0031	42	0.1234

Table 3.10: HCN capture.

Test	HCN capture (g/L/hr)
1	$1.56x10^{-7}$
2	$2.025x10^{-6}$
3	$8.125x10^{-7}$
4	$1.016x10^{-6}$
5	$4.063x10^{-7}$

Table 3.11: Emissions test variables and ranges examined.

Test ID	A/m^2	Temp (°C)	CN ppm	NaOH (g/L)	NH_3 (L/hr)	CN loss (g/hr)
ET 1	30	88	**500**	10	0.047	0.258
ET 2	30	88	**1000**	10	0.099	0.520
ET 3	30	88	**2000**	10	0.202	1.105
ET 4	30	88	**4000**	10	0.392	2.340
ET 5	30	88	1000	10	0.151	0.780
ET 6	30	**71**	1000	**20**	0.098	0.520
ET 7	30	**71**	1000	10	0.045	0.260
ET 8	30	**71**	**4000**	10	0.185	1.040
ET 9	30	88	1000	10	0.090	0.520
ET 10	30	88	1000	**5**	0.049	0.260
ET 11	30	88	1000	10	0.090	0.449
ET 12	30	88	1000	**15**	0.084	0.520
ET 13	30	88	1000	**20**	0.140	0.780
ET 14	**20**	88	1000	10	0.087	0.520
ET 15	**25**	88	1000	10	0.125	0.650
ET 16	**35**	88	1000	10	0.106	0.780

Table 3.12: Comparison of cyanide loss with and without electrolysis.

CN (ppm)	Temp (°C)	CN loss with e- (g/hr)	CN loss without e- (g/hr)
500	88	0.26	0.3
2000	88	1.64	1.04
4000	88	2.50	2.08
2000	55	0.26	0.17

4 DISCUSSION

4.1 Anode Corrosion

4.1.1 Effect of NaCN

Linear regression analysis was performed using Microsoft Excel after first discarding a few outlying data points. Figure 4.1 shows the graph and the relationship between cyanide concentration and corrosion. The P-value is less than the significance level α which was chosen to be 0.05. This indicates that there is a linear relationship between corrosion and cyanide. The margin of error was calculated to be 0.043. The margin of error is the radius of the confidence interval for the equation given in Figure 4.1. The margin of error is fairly high due to the variability in the data. Table 4.1 shows the margin of error which represents the radius of the confidence interval. When the P-value < α (0.05) there is a corresponding relationship between the input and response variables.

The addition of free cyanide ions to electrowinning process has been reported to have a negative effect on cell performance. Brandon et al. found that when the concentration of free cyanide ions was increased the recovery of gold decreased. This was attributed to a cathodic shift in the reversible potential for gold deposition. High recovery was reported when using dilute cyanide leach liquors (Brandon 1987). The relationship with corrosion and recovery indicate that when it comes to cyanide less is more.

4.1.2 Effect of NaCl

The relationship of sodium chloride and corrosion is shown in Figure 4.2 while statistical data are shown in Table 4.2. The P-value is greater than 0.05, therefore sodium chloride does not show a significant linear relationship with corrosion rate. This, however, does not indicate that sodium chloride does not cause corrosion. This does not agree with the study done by Maier and Frankel, however, the concentrations are lower in this study. It is possible that at low concentrations chlorides do not have a significant relationship with corrosion while at high concentrations they do. Pitting corrosion is caused by halide salts and chloride is the most active cause of pitting corrosion. While the mass loss is not extensive it can be deep causing stress fractures and failure. Pitting corrosion is agued by some to be the most expensive type of corrosion (Newman 2010).

The depth of the pit in Figure 3.7 is 10 microns while the thickness of the anode is 500 micron. If the corrosion continued at the same rate the anode could be expected to fail in 300 weeks if not less. If the corrosion were to occur on both sides of the anode the time to failure would be 150 weeks. Studies have shown that corrosion caused by chlorides takes place in three stages: an incubation period, a rapid development stage and a stable development stage. The corrosion will continue at a steady rate once the stable development stage has been reached (Hu 2011).

4.1.3 Effect of NaOH

The relationship between NaOH and corrosion is shown in Figure 4.3, and the statistical data in Table 4.3. The P-value is greater than 0.05, therefore NaOH does not show a significant linear relationship with corrosion. The literature available on the subject of hydroxide and corrosion indicates stainless steel resists corrosion by hydroxide

at mild temperatures (Craig 1995). Less weight loss has been reported in more alkaline solutions; however, the temperature was not reported (Shreir 1963). The resistance to corrosion was not seen in this study; however, this could be because of the higher temperature utilized.

The pitting observed in the tests with varied NaCl was not observed in the NaOH tests. It is apparent the corrosion caused by NaOH is more uniform over the entire surface of the anode than that observed in the sodium chloride tests. Gold was not used in these experiments, however, it is interesting to note that Brandon et al. found higher gold recovery in electrolyte solutions of a higher pH. pH values of 10, 11, 12, 13 and 14 were tested and the recovery was greatest in the solution with a pH of 13. The solution with a pH of 14 showed an equivalent recovery to that of pH 13 (Brandon 1987).

4.1.4 Effect of Current Density

Figure 4.4 shows the relationship between current density in the anode and corrosion of the anode. Table 4.4 contains the statistical data. Because the P-value is greater than 0.05 the linear relationship is not statistically significant. Moskalyk et al. found that higher current densities may cause particles to flake off the anode causing uneven distribution of current throughout the electrode. When the current density is uneven in the anode, areas of high and low current are created in the cathode. Uneven current density causes low current efficiency and lower quality of the metal plating. Costello et al. also observed that high current densities can cause poor plating in gold and cause codeposition of other species, including the generation of hydrogen gas (Costello 2005). Perhaps the corrosion is slightly lower because of extra hydrogen bubbles on the anode.

4.1.5 Effect of Silica

Figure 4.5 shows the effect of silica on corrosion. The P-value of the regression analysis shown in Table 4.5 is very small which indicates there is a linear relationship between silica and corrosion. The margin of error is fairly large due to the variability of the samples. The graph indicates that between 1.5 and 2.0 g/L Na_2SiO_3 the corrosion rate increases, while less than 1.5 g/L the corrosion is close to zero. In the literature silica is reported to inhibit corrosion measured by mass loss. Silica is used to increase resistivity in concrete, protecting the steel reinforcement bars from corrosion (Dotto 2004).

Silica is also added to water systems to inhibit corrosion in pipes because it slows oxidation, however, increased silica concentration also leads to the increase of particulate iron in solution (Rushing 2003). Dense layers of ferrous hydroxide and iron oxides were found in iron exposed to silica rich solutions (Cekerevac 2012). In this study tubercles were prevalent on the samples with large corrosion; these tubercles contributed to mass gain in some cases and fell off during electrode cleaning. The samples with low silica content did not have tubercles. This study indicates that while silicate may be a corrosion inhibitor at low concentrations, at high concentrations it increases the rate of corrosion through the formation of tubercles. Table 4.5 shows the P-value indicates a linear relationship, the margin of error, however, is large.

4.1.6 Effect of Sulfate

Figures 4.6 and 4.7 both show the relationship of sulfate with corrosion. Figure 4.6 shows the data for both high and low concentrations of sulfate. Figure 4.7 better shows the relationship between the low sulfate concentrations and corrosion. The P-value shown in Table 4.6 indicates that there is a strong linear relationship between sulfate and

corrosion. Sulfate ions are especially corrosive to the water line (Shreir 1963). In Figure 3.8 the anodes from the sulfate test are shown. There were three anodes that corroded so much on the water line the anode completely broke off. Concentrations greater than 0.25 grams per liter of sodium sulfate in the electrolyte show a rapid increase in the corrosion rate. The study indicates that if the sodium sulfate concentration is kept at 0.25 grams per liter or less the corrosion will still happen but the rate would not be expected to increase dramatically.

Tubercles formed on the anodes exposed to high levels of sulfate just as they did in solutions with high levels of silica. Shreir (1963) reports acceleration in corrosion rate with the formation of tubercles. The tubercles act as a cathode and traps acid formed by the oxidation of the iron further oxidizing the anode. Black precipitate was noted at the bottom of electrowinning cells containing high concentrations of sulfate. Smith et al. also reports observation of a black precipitate which was identified as Ferrous oxide.

4.1.7 Effect of Mixed Sulfate and Silica

The most corrosion was observed with sodium sulfate, however, there was a much higher concentration used than that in the highest sodium silicate concentration test. Figure 4.8 shows both predicted lines plotted together. The slopes of the regression lines indicate that silica causes a greater increase in the rate of corrosion as concentration increases than any other ion. Figure 4.8 also suggests that concentrations lower than about 1.1 g/L Na_2SO_4 cause a greater corrosion rate. Concentrations higher than about 1.1 g/L Na_2SiO_3 are the greatest contributor to the corrosion rate.

4.1.8 Effect of Temperature

Temperature has been shown to both increase and decrease the rate of corrosion (Craig 1995) (Rushing 2003). Temperature influences many parameters in solutions such as dissolved oxygen, activity coefficients, and oxidation rates. All of these factors influence corrosion of iron. In this study the temperature always promoted corrosion. The effects of temperature on both a high and low concentration of sulfate and silica respectively were tested and plotted in Figure 4.9. The plot indicates that when the concentration of sulfate is high the rate of corrosion increases significantly between 76 and 82 °C. However, the corrosion rate was about the same between 82 and 88 °C. For lower concentrations the rate increases between 82 and 88 °C.

A similar trend is found in the Figure 4.10 which is a plot of temperature and corrosion at a high and low concentration of silica. The increase in the rate of corrosion is observed between 83 and 88 °C for both the high and low level of silicate. However, the high level of silicate shows a much larger increase. The data indicate silicate will cause a higher corrosion rate as the concentration increases. Both graphs indicate that when electrowinning is conducted at approximately 75 ^{o}C or lower the effect of the ions decreases dramatically. In processes where the ions in solution are hard to control a good method of decreasing corrosion may be to keep the temperature below 75 ^{o}C.

4.2 Emission Test

4.2.1 Ammonia Emission and Cyanide Loss

The main factor corresponding to emission of ammonia gas was identified to be the amount of cyanide degradation. Figure 4.11 shows a linear relationship between ammonia capture and cyanide degradation. This relationship appears to be independent

of temperature within the range studied (88-71°C). The ammonia captured varied between 18 to 23 % of the amount of ammonia for stoichiometric consumption of cyanide. Dzombak et al. lists ammonia and formate as the products of cyanide decomposition from electrolysis. The parameters examined showed an effect on ammonia generation only in that the parameters influenced the cyanide degradation, which was found to always be proportional to ammonia generation. In order to avoid errors from leaks in the testing apparatus, the effect of the test parameters will be compared to the amount of cyanide lost rather than the ammonia captured. The P-value found in Table 4.7 associated with the regression line is much less than 0.05 indicating a very good fit; the margin of error supports this conclusion. The red marks indicate 88 °C, and blue indicates 71 °C.

4.2.2 Cyanide Concentration vs. Cyanide Loss

The effect of cyanide concentration as well as temperature is illustrated in Figure 4.12. Higher temperature corresponded to greater cyanide loss for all cyanide concentrations tested. With higher concentration of cyanide the difference between the two temperatures tested grows more pronounced. Dzombak et al. report higher rates of cyanide degradation with higher temperature and higher pressure. Table 4.8 shows the error associated with the slope of the higher temperature cyanide concentration to cyanide loss relationship. Because there are only two points at 71 °C, errors cannot be calculated. The P-value of the 88 °C tests is less than 0.05 indicating there is a linear relationship. The margin of error is fairly low, indicating this line is a good fit.

4.2.3 Hydroxide Concentration and Cyanide Loss

Figure 4.13 shows the increasing rate of cyanide loss with sodium hydroxide, again the effect of temperature is evident. The P-value presented in Table 4.9 is slightly larger than 0.05 indicating that the relationship is not statistically significant. However, Cheng et al. (2002) when observing a wider range of pH values, found that oxidation of cyanide occurs more rapidly at higher hydroxide concentrations.

4.2.4 Current Density and Cyanide Loss

The relationship of current density with CN^- loss is shown in Figure 4.14. It appears that current density has a positive correlation with CN^- loss; however, the P-value shown in Table 4.10 indicates the linear relationship is not statistically significant.

Comparing mass loss of cyanide with and without electrolysis indicates that the mass loss is largely due to heat. Linear regression as shown in Figure 4.15 predicts a slightly greater rate of cyanide loss for tests with electrolysis than those without. The results indicate the main factor contributing to cyanide degradation is hydrolysis and not electrolysis. The effect of electrolysis on cyanide mass loss increased with greater initial cyanide concentration. Ho et al. found that cyanide concentration can be dramatically reduced by using electrolysis; the current and temperature were not given, however.

Figure 4.16 shows the data for the effect of temperature and electrolysis on cyanide mass loss. The cyanide concentration for all data in Figure 4.16 is 2000 ppm. Higher temperatures yielded a larger difference in cyanide loss between tests with and without electrolysis.

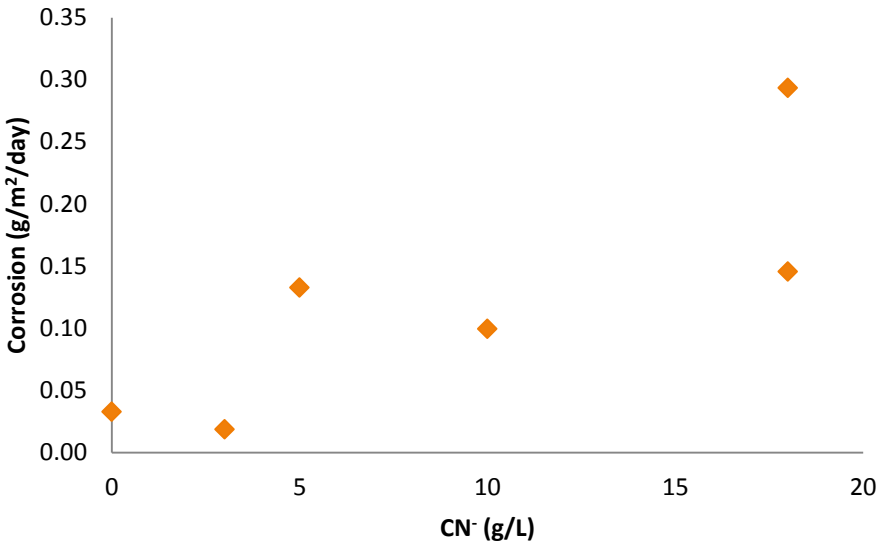

Figure 4.1: Cyanide vs. corrosion, data taken from Table 3.1 and test 48 in Table 3.7.

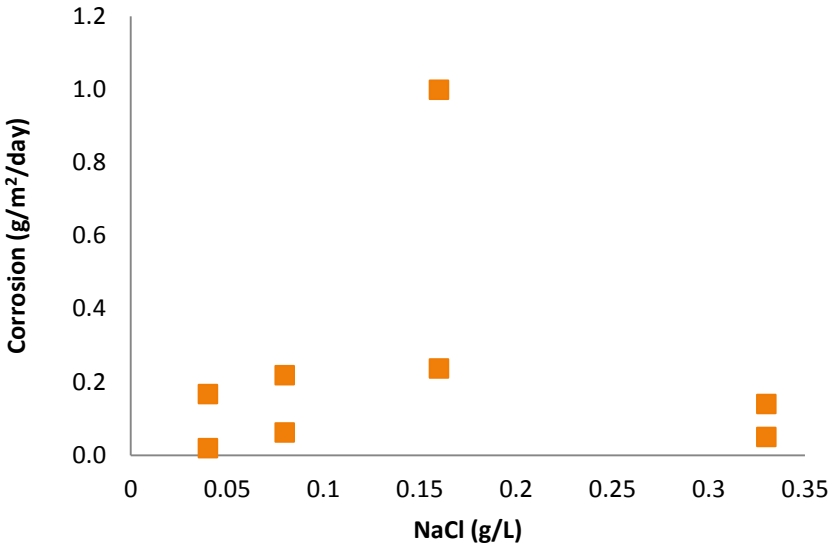

Figure 4.2: The relationship between chloride and corrosion, data taken from Table 3.2.

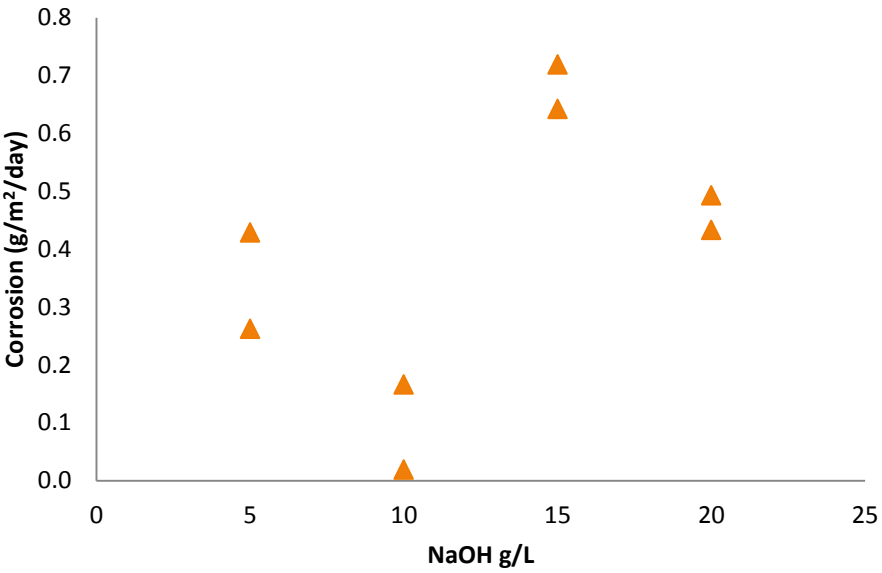

Figure 4.3: NaOH vs. corrosion, data taken from Table 3.4.

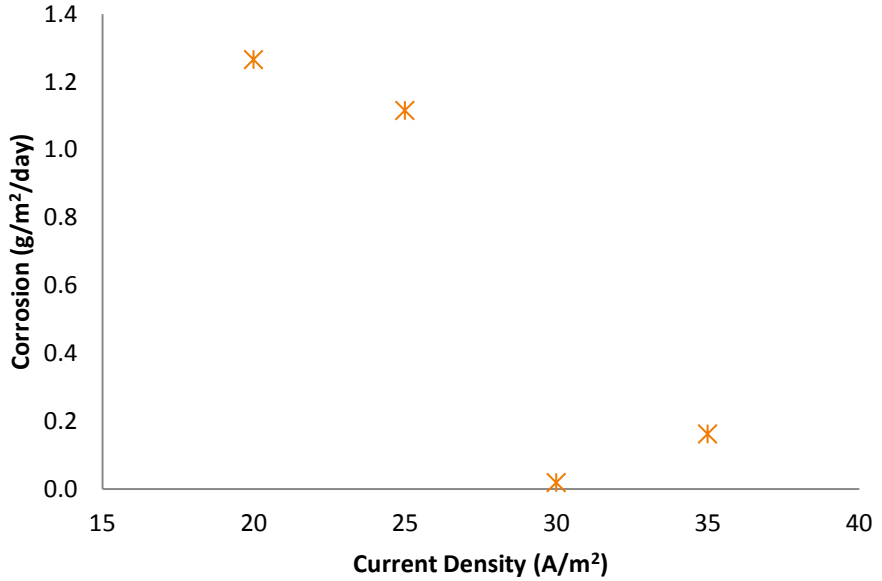

Figure 4.4: Current density vs. corrosion, data taken from Tables 3.2 and 3.5.

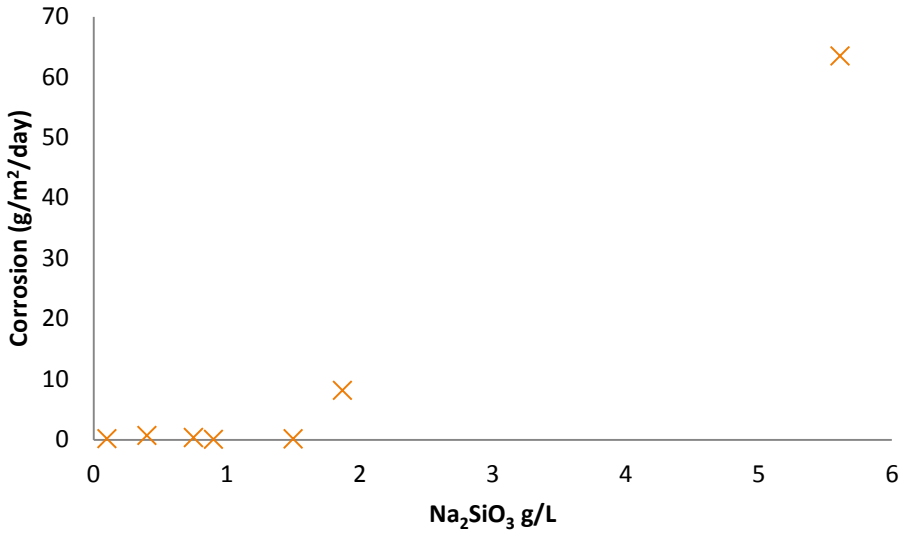

Figure 4.5: The relationship of Na_2SiO_3 with corrosion, data from Tables 3.5, 3.7, 3.9.

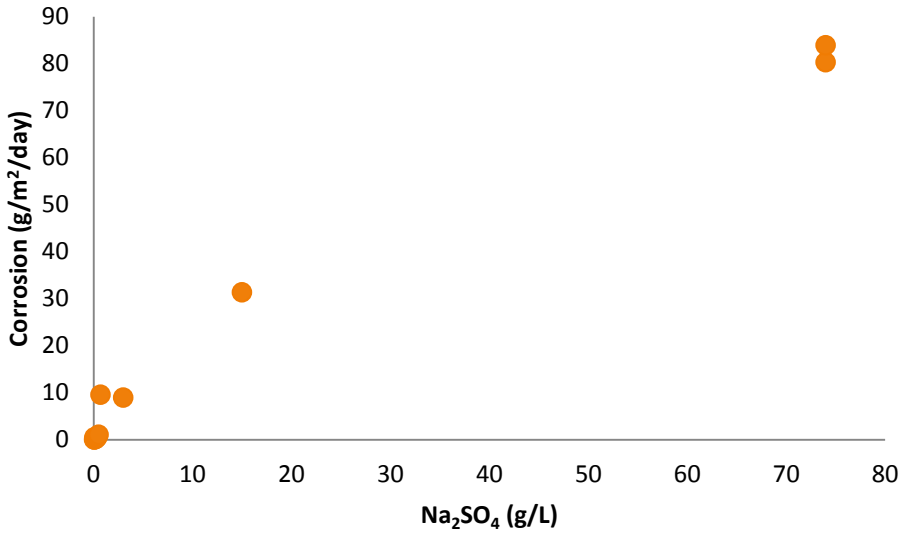

Figure 4.6: The effect of Na_2SO_4 on corrosion, data from Tables 3.3, 3.7, and 3.9.

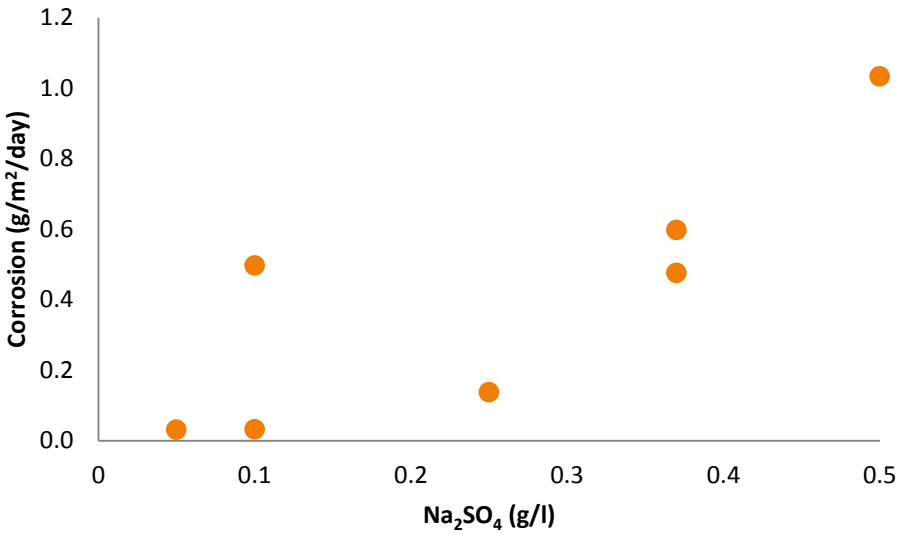

Figure 4.7: Na_2SO_4 concentration values less than 0.5 g/L, data from Tables 3.7 and 3.9.

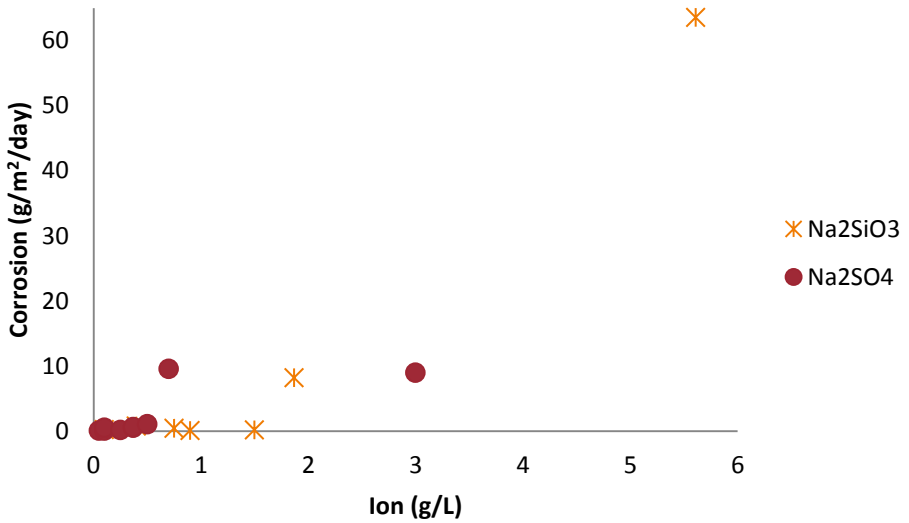

Figure 4.8: The effect of Na_2SO_4 and Na_2SiO_3, data from Tables 3.3, 3.5, 3.7, and 3.9.

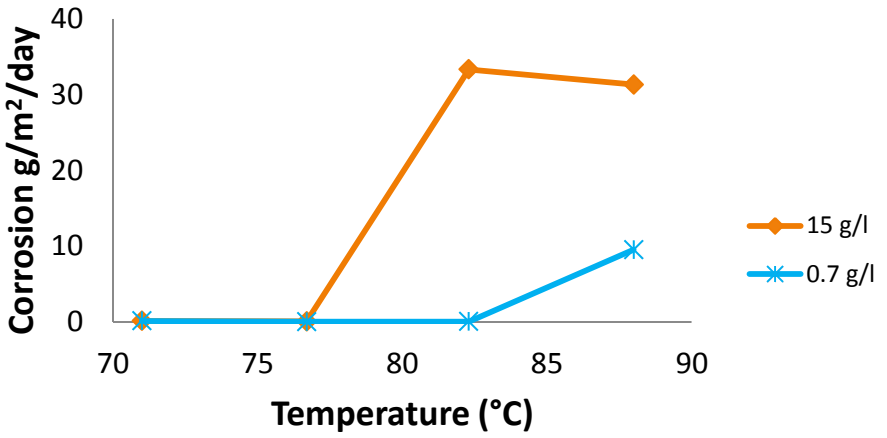

Figure 4.9: Na_2SO_4 at various temperatures, data from Tables 3.3 and 3.8.

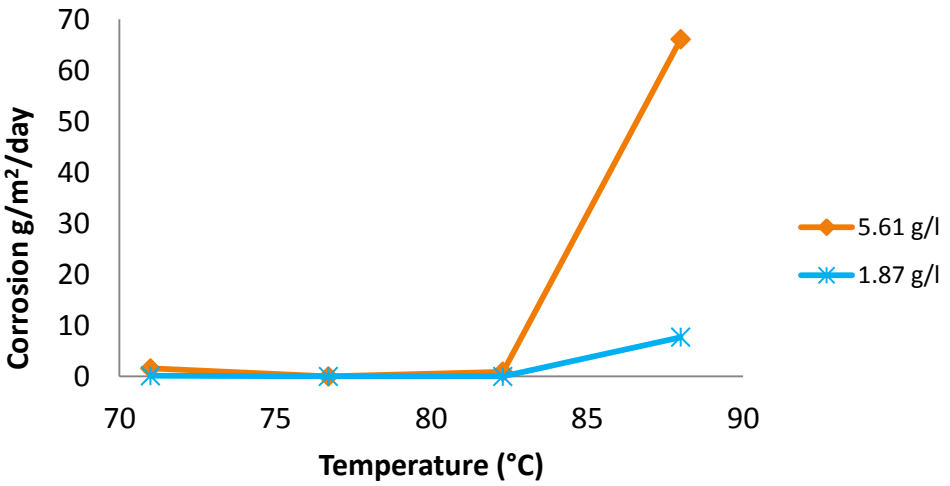

Figure 4.10: Na_2SiO_3 corrosion rate compared to temperature, data from Tables 3.4 and 3.8

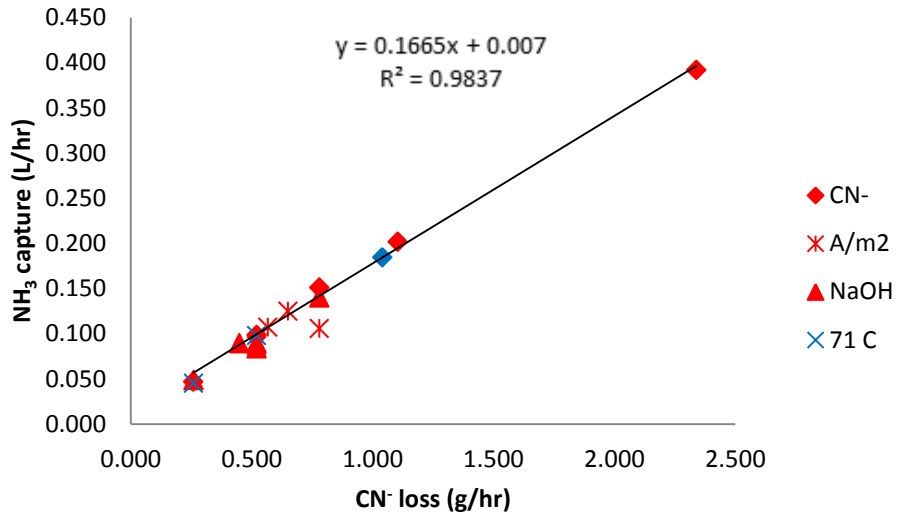

Figure 4.11: Cyanide loss vs. ammonia capture for all tests, data from Table 3.11.

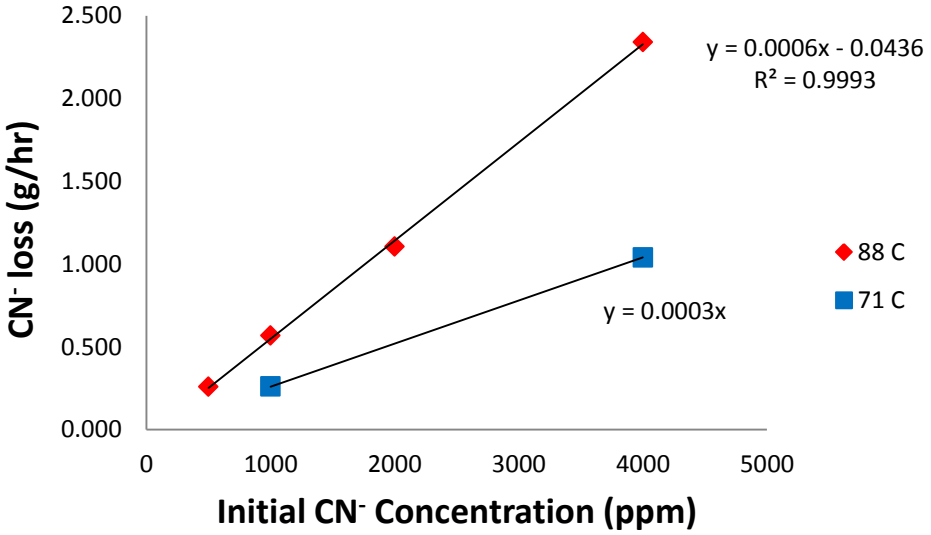

Figure 4.12: Initial CN^- concentration vs. CN^- loss, data from Table 3.11 ET 1-4, 7, and 8.

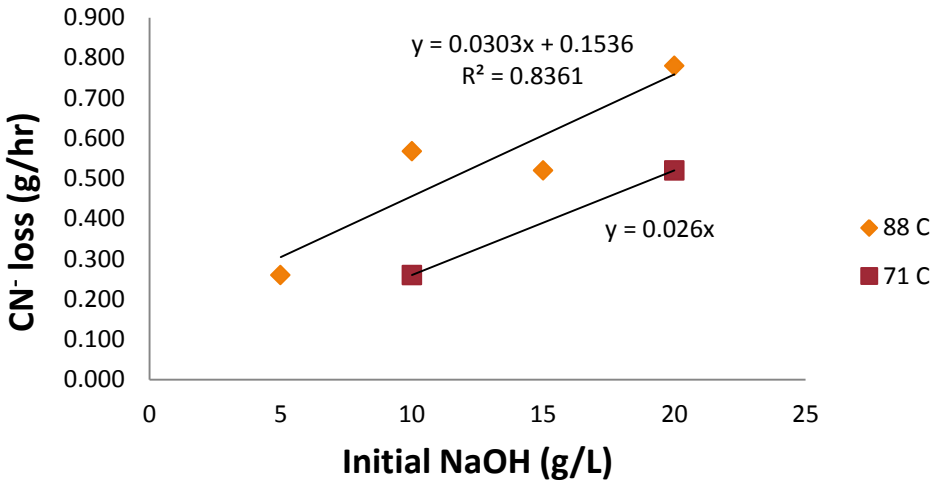

Figure 4.13: CN^- loss compared to NaOH, data from Table 3.11 ET 10-13, 6, and 7.

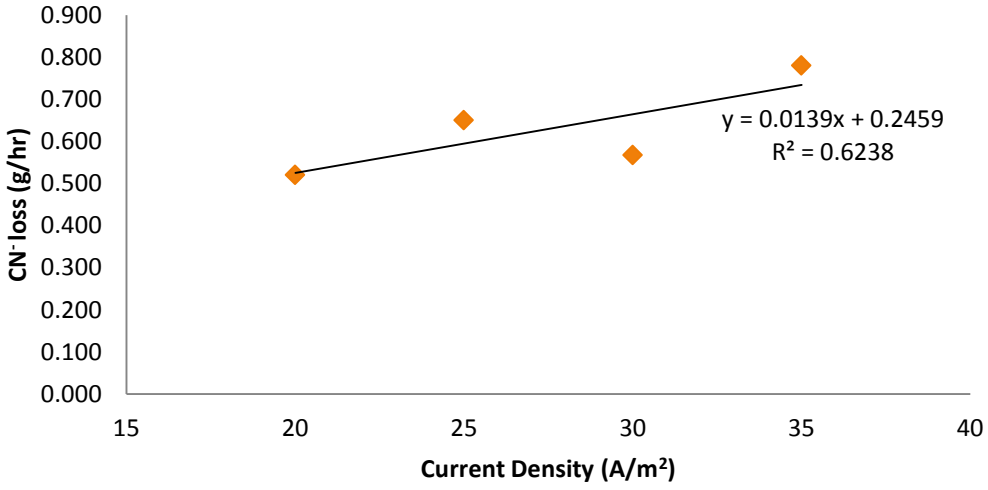

Figure 4.14: Current density and CN^- loss, data from Table 3.11 ET 14-16.

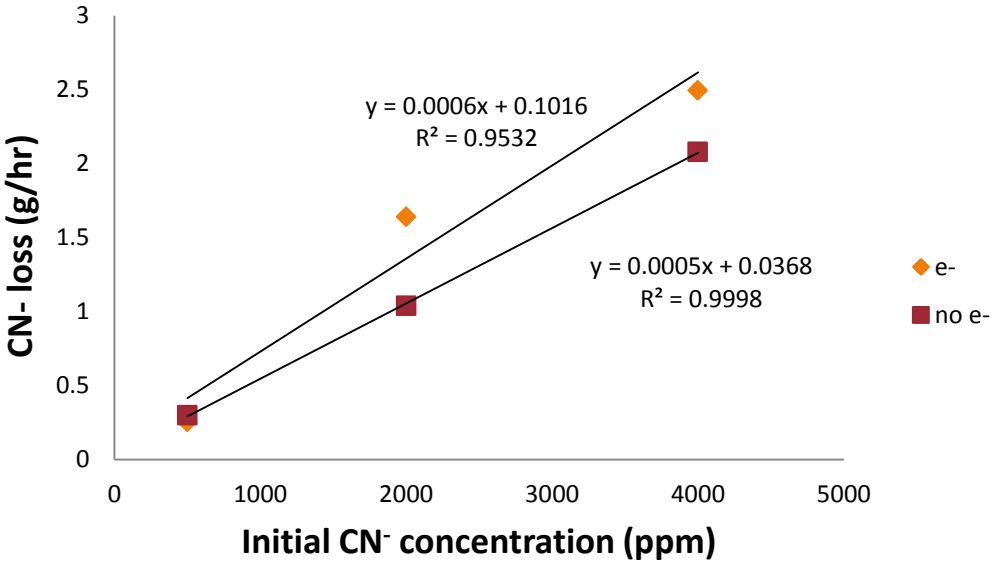

Figure 4.15: CN^- loss with and without electrolysis, data from Table 3.12.

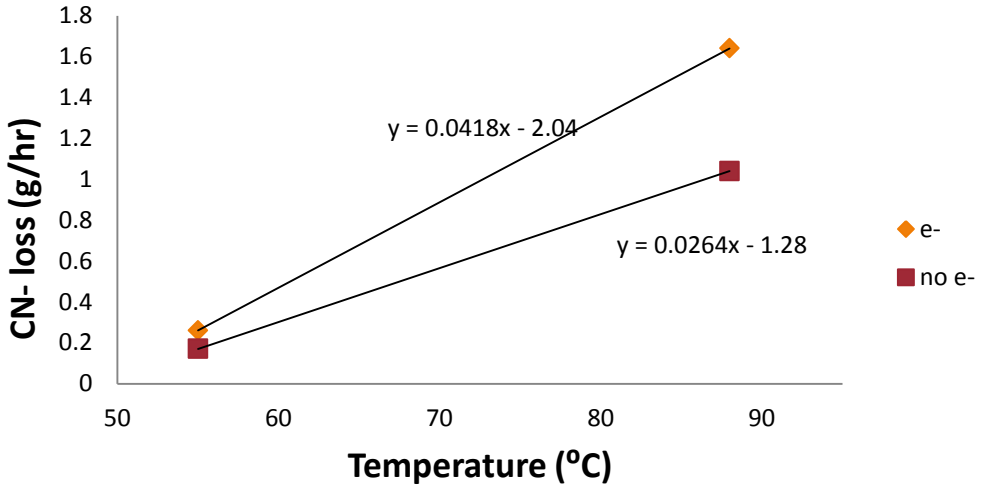

Figure 4.16: CN^- loss vs. temperature, data from Table 3.12.

Table 4.1: Statistics for Figure 4.1.

	Margin of Error	*P-value*
NaCN	0.043	0.029

Table 4.2: The error of the relationship in Figure 4.2.

	Margin of Error	*P-value*
NaCl	0.076	0.995

Table 4.3: The error associated with Figure 4.3.

	Margin of Error	*P-value*
NaOH	0.166	0.308

Table 4.4: The error in Figure 4.4.

	Margin of Error	*P-value*
A/m2	0.295	0.112

Table 4.5: The error associated with Figure 4.5.

	Margin of Error	*P-value*
Na_2SiO_3	4.851	4.0E-04

Table 4.6: The error associated with Figure 4.6.

	Margin of Error	*P-value*
Na_2SO_4	3.682	1.29E-08

Table 4.7: The error associated with Figure 4.11.

	Margin of Error	*P-value*
CN loss (g/hr)	0.0075	8.063E-15

Table 4.8: The error associated with Figure 4.12.

	Margin of Error	*P-value*
Initial CN^- (ppm)	0.0250	0.0004

Table 4.9: The error associated with Figure 4.13.

	Margin of Error	*P-value*
NaOH (g/L)	0.0865	0.0856

Table 4.10: The error associated with Figure 4.14.

	Margin of Error	*P-value*
A/m^2	0.0699	0.210167

5 CONCLUSIONS

The data indicate that the greatest cause of increased corrosion rate is temperature. Temperatures of 76.7 ^{o}C or less did not cause corrosion greater than 0.5 g/m^2/day except in the case of anode 47 which had high cyanide and high silica; the corrosion was 1.5 g/m^2/day in that case. At 88 ^{o}C the greatest contributor to increased corrosion rate was silica at concentrations greater than 1 g/L. Silica is reported as being a corrosion inhibitor, and at low concentrations large corrosion rates were not observed. The mixture of silica and sulfate did show lower corrosion rates than those of sulfate at the same concentration. Sulfate concentrations less than 1 g/L showed sulfate as the greatest contributor to corrosion rate. Cyanide concentration had a small effect on corrosion rate.

Corrosion was observed at varied current density, chloride, and hydroxide, however, there was not a significant linear relationship. While chloride did not show a significant linear relationship with corrosion, pitting was observed in samples with larger chloride concentration, which is a concern in industry. Other studies examining the effect of chlorides at a greater concentration have shown a relationship between chloride concentration and corrosion. It is possible this study examined only concentrations below a threshold where chlorides begin to show significant trends.

The amount of ammonia evolved from the electrowinning cell was found to be directly proportional to the amount of cyanide loss in any given test. The largest

contributor to cyanide destruction was temperature and cyanide concentration. The effects of hydroxide and current density were small. The evolution of hydrogen cyanide gas was found to be negligible.

APPENDIX

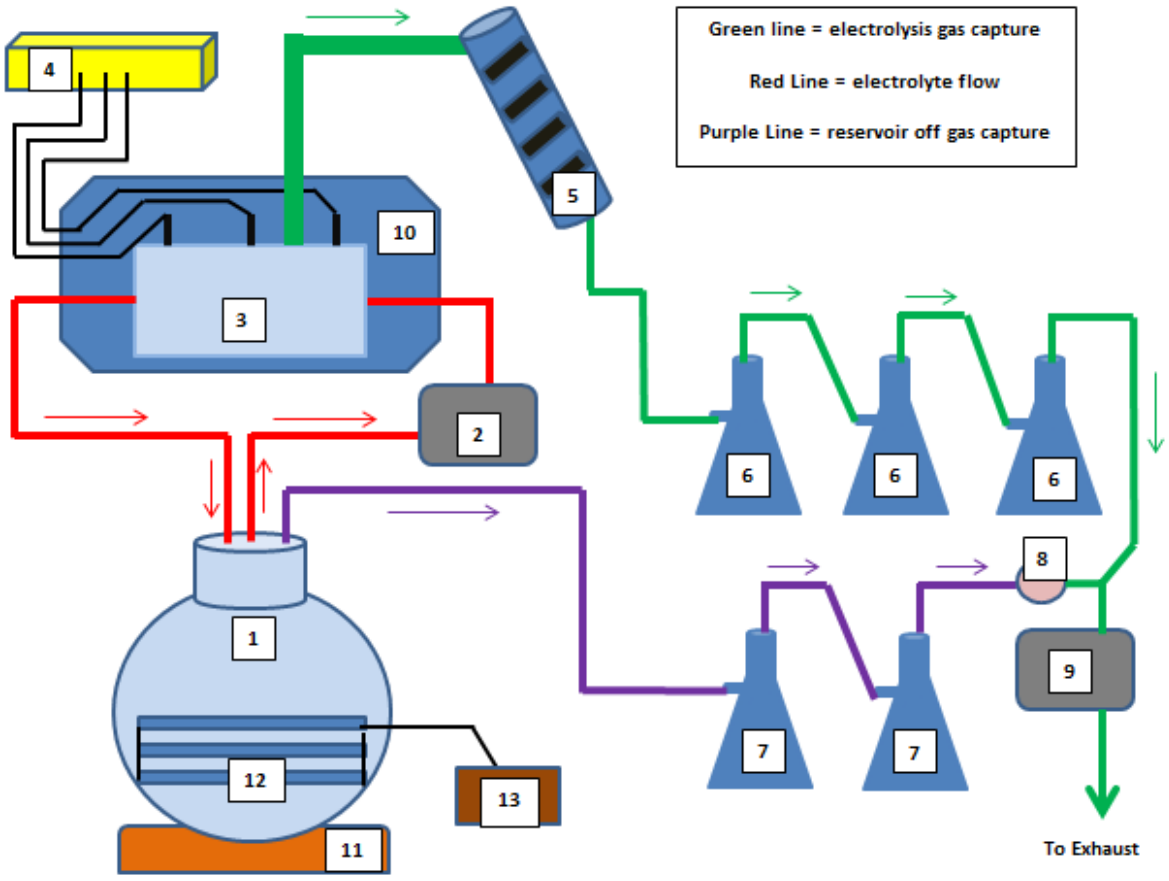

1. 20 liter solution reservoir
2. Peristaltic pump (for electrolyte)
3. Electrolysis cell (middle electrode is the anode, the outer two are cathodes)
4. Power supply
5. Condenser

6. Erlenmeyer flask, 500ml, equipped with fritted glass spargers for electrolysis off gas capture; flask filled with glass beads for improved performance
7. Identical flask setup as “6” for the purpose of capturing reservoir off gasses
8. Valve to control gas flow
9. Peristaltic pump (for gas)
10. Gas containment cell (for increased gas flow stability)
11. Heating plate
12. Adjustable temperature heating tape

REFERENCES

Agency for Toxic Substance and Disease Registry. ToxFAQs for Ammonia. 2004. http://www.atsdr.cdc.gov/toxfaqs/tf.asp?id=10&tid=2 (accessed September 2013).

ASTM. Standard Practice for Preparing, Cleaning, and Evaluating Corrosion Test Specimen. Standard, Conshohocken: ASTM International, 2003.

Blount, B. Practical Electro-Chemistry. London: Archibald Constable & Co LTD, 1906.

Brandon, N.P., Mahmood, M.N., Page, P.W., Roberts, C.A. "The Direct Electrowinning of Gold from Dilute Cyanide Leach Liquors." Hydrometallurgy, 1987: 305-319.

Busch, D.A., Stone, J.R., Chiszar, G. "Production of Refined Nickel Sulfate at Asareo's Perth Amboy Plant." In Extractive Metallurgy of Copper, Nickel, and Coblat, by P. Queneau, 469. New York: American Institute of Mining, Metallurgical and Petrolium Engineers, 1961.

Cekerevac, M., Simicic, M., Bujanovic, L.N., Popovic, N. "The Influence of Silicate and sulfate Anions on the Anodic Corrosion and the Transpassivity of Iron and Silicon Rich Steel in Concentrated KOH Solution." Corrosion Science, 2012: 204-212.

Chandler, H. Metallurgy for the Non-Metallugist. Materials Park: ASM International, 1998.

Cheng, S.C., Gattrell, M., Guena, T., MacDougall, B. "The Electrochemical Oxidation of Alkaline Copper Cyanide Solutions." Electrochimica Acta, 2002: 3245-3256.

Colorado State University. Best Management Practices . June 20, 2008. ammoniabmp.colostate.edu/link%20pages/impacts%20of%20ammonia.html (accessed September 2013).

Costello, M. "Electrowinning: Advances in Gold Ore Processing." Developments in Mineral Processing, 2005: 15.

Craig, B.D., Anderson, D. S. Handbook of Corrosion Data Second Edition. Materials Park: ASM International, 1995.

Dotto, J.M.R., De Abreu, A.G., Dal Molin, D.C.C., Müller I.L. "Influence of Silica Fume addition on Concrete's Physical Properties and on Corrosion Behaviour of Reinforcement Bars." Cement and Concrete Composites, 2004: 31-39.

Dzombak, D., Ghosh, R.S., Young, T.C. "Physical-Chemical Properties and Reactivity of Cyanide in Water and Soil." In Cyanide in Water and Soil, by D.A., Ghosh, R.S., Wong-Chong, G.M. Dzombak, 58-88. Boca Raton: Taylor & Francis Group, 2006.

Dzombak, D.A., ghosh, R.S., Wong-Chong, G.M. Cyanide in Water and Soil: Chemistry Risk, Management. Boca Raton: Taylor & Francis Group, 2006.

Ettel, V.A., Gendron, A.S., Tilak, B.V. "Electrowinning Copper at High Current Densities." Metallurgical and Material Transactions, 1975: 31-36.

Fontana, M. G. Corrosion Engineering 3rd ed. New York: McGraw-Hill, 1986.
Gupta, C.K., Mukherjee, T.K. Hydrometallurgy in Extration Process Volume 2. Boca Raton: CRC Press, 1990.

Harris, D.C. Quantitative Chemical Analysis. New York: Michelle Russel Julet, 2003.

Hays, G.F. "The World Corrosion Organization." Raising Awareness About Corrosion and Corrosion Protection Around the World. 2013. http://www.corrosion.org (accessed October 4, 2013).

Higham, T., Chapman, J., Slavchev, V., Gaydarska, B., Honch, N., Yordanov, Y., Dimitova B. "New Perspectives On the Varna Cemetery (Bulgaria)." Antiquity, 2007.

Ho, S.P., Wang, Y.Y., Wan, C.C. "Electrolytic Decomposition of Cyanide Effluent with an Electrochemicla Reactor Packed with Stainless Steel Fiber." Water Research, 1990: 1317-1321.

Hu, Q., Zhang, G., Qiu, Y., Guo, X. "The Crevice Corrosion Behaviour of Stainless Steel in Sodium Chloride Solution." Corrosion Science, 2011: 4065-4072.

International Cyanide Management Institute. Cyanide Code. 2012. http://www.cyanidecode.org/cyanide-facts/cyanide-chemistry (accessed August 2013).

Litz, J.E. "Solvent Extraction of W, Mo, and V: Similarities and Contrasts." In Extractive Metallurgy of Refractory Metals, by H.Y., Carlson, O.N., Smith, J.T. Sohn, 69. New York: The Metallurgical Society of AIME, 1981.

Maier, B., Frankel, G.S. "Pitting Corrosion of Bare Stainless Steel 304 under Chloride Solution Droplets." Journal of the Electrochemical Society, 2010: C302-C312.

Mallan, L. Suiting Up For Space: The Evolution of the Space Suit. John Day Co., 1971.

McMaster-Carr. McMaster-Carr. n.d. http://mcmaster.com/#standard-type-304-stainless-steel-sheets/=oheffa (accessed March 2013).

Moskalyk, R.R, Alfantzai, A., Tombalakian, A.S., Valic, D. "Anode Effects in Electrowinning." Minerals Engineering, 1999: 65-73.

Mulvaney, P. "The Beauty and Elegance of Nanocrystals: How Invisibly Small Particles Will Colour and Shape Our Future." University News: The University of Melbourne, July 28, 2003.

Newman, R. "Pitting Corrosion of Metals." Journal of The Electrochemical Society, 2010: 33-38.

Phillips, R.W. Skinner's Science of Dental Materials. Philadelphia: W.B. Sauners Co., 1986.

Pistorius, P.C., Burstein, G.T. "Metastable Pitting Corrosion of Stainless Steel and the Transition to Stability." Philosophical Transactions of the Royal Society of London Series A: Physical and Engineering Sciences, 1992: 531-559.

Qian, X. "In Vivo Tumor Targeting and Spectroscopic Detection with Surface-Enhanced Raman Nanoparticle Tags." Nature Biotechnology, 2008.

Rushing, Jason C., McNeil, Laurrie S., Edwards, Marc. "Some Effects of Aqueous Silica on the Corrosion of Iron." Water Reaserch, 2003: 1080-1090.

Shreir, L.L. Corrosion. London: George Newness LTD, 1963.

Simard, S., Odziemkowski, M., Irish, D.E., Brossard, L., Menard, H. "In Situ Micro-Ramen Spectroscopy to Investigate Pitting Corrosion Product of 1024 Mild Steel in Phosphate and Bicarbonate Solutions Containing Chloride and Sulfate Ions." Journal of Applied Electrochimistry, 2001: 913-920.

Smith, P., Roy, S., Swailes, D., Maxwell, S., Page, D., Lawson, J. "A Model for the Corrosion of Steel Subjected to Synthetic Produced Water Containing Sulfate, Chlorine and Hydrogen Sulfide." Chemical Engineering Science, 2011: 5775-5790.

University of Sheffield. Web Elements. 1993. http://www.webelements.com/gold/ (accessed May 2013).

Valiūnienė, A., Baltrūnas, G., Keršulytė, V., Margarian, Ž., Valinčius, G. "The Degradation of Cyanide by Anodic Electro oxidation Using Different Anode Materials." Process Safety and Environmental Protection, July 2013: 269-274.

World Health Organisation. Hydrogen Cyanide and Cyanides: Human Health Aspects. Concise International Assessment Document 61, World Health Organisation, 2004.

Yang, L., Wei, Y., Hou, L., Zhang, D. "Corrosion Behaviour of Die-cast AZ91D Magnesium Alloy in Aqueous Sulphate Solutions." Corrosion Science, 2010: 345-351.

Yannopoulos, J.C. The Extractive Metallurgy of Gold. New York: Van Nostrand Reinhold, 1991.